Chapter 2 Galactic Gamma-ray Sources*

Yang Chen(陈阳)[1★¶‡] Xiao-Jun Bi(毕效军)[2¶] Kun Fang(方堃)[2¶] Yi-Qing Guo(郭义庆)[2¶] Ye Liu(刘烨)[3¶]
P. H. Thomas Tam(谭柏轩)[4¶] S. Vernetto[5¶] Zhong-Xiang Wang(王仲翔)[6¶] Rui-Zhi Yang(杨睿智)[7,8,9¶]
Xiao Zhang(张潇)[1★¶†]

[1]School of Astronomy and Space Science, Nanjing University, Nanjing 210023, China
[2]Key Laboratory of Particle Astrophysics, Institute of High Energy Physics, CAS, P.O. Box 918, Beijing 100049, China
[3]School of Management Science and Engineering, Hebei University of Economics and Business, Shijiazhuang, Hebei 050061, China
[4]School of Physics and Astronomy, Sun Yat-Sen University, Guangzhou 510275, China
[5]Istituto Nazionale di Astrofisica, OATO, Torino, Italy
[6]Key Laboratory for Research in Galaxies and Cosmology, Shanghai Astronomical Observatory, Chinese Academy of Sciences, 80 Nandan Road, Shanghai 200030, China
[7]Department of Astronomy, School of Physical Sciences, University of Science and Technology of China, Hefe 230026, China
[8]CAS Key Laboratory for Research in Galaxies and Cosmology, University of Science and Technology of China, Hefei 230026, China
[9]School of Astronomy and Space Science, University of Science and Technology of China, Hefei 230026, China

Abstract: In the γ-ray sky, the highest fluxes come from Galactic sources: supernova remnants (SNRs), pulsars and pulsar wind nebulae, star forming regions, binaries and micro-quasars, giant molecular clouds, Galactic center, and the large extended area around the Galactic plane. The radiation mechanisms of γ-ray emission and the physics of the emitting particles, such as the origin, acceleration, and propagation, are of very high astrophysical significance. A variety of theoretical models have been suggested for the relevant physics, and emission with energies $E\geq10^{14}$ eV are expected to be crucial in testing them. In particular, this energy band is a direct window to test at which maximum energy a particle can be accelerated in the Galactic sources and whether the most probable source candidates such as Galactic center and SNRs are "PeVatrons". Designed aiming at the very high energy (VHE, >100 GeV) observation, LHAASO will be a very powerful instrument in these astrophysical studies. Over the past decade, great advances have been made in the VHE γ-ray astronomy. More than 170 VHE γ-ray sources have been observed, and among them, 42 Galactic sources fall in the LHAASO field-of-view. With a sensitivity of 10 milli-Crab, LHAASO can not only provide accurate spectra for the known γ-ray sources, but also search for new TeV-PeV γ-ray sources. In the following sub-sections, the observation of all the Galactic sources with LHAASO will be discussed in details.

Keywords: γ-rays, cosmic rays, radiation mechanisms, PeVatrons

DOI: 10.1088/1674-1137/ac3fa8

I. INTRODUCTION

During the last twenty years, the achievements in γ-ray astronomy both in the GeV energy range with space borne instruments (like EGRET, AGILE, and Fermi) and in the TeV region with ground based detectors (like Whipple, H.E.S.S., MAGIC, VERITAS, MILAGRO, and ARGO-YBJ), produced extraordinary advances in high energy astrophysics, with the detection of a large number of sources (more than 5000 in the Fermi catalogue), about 170 of which emitting up to TeV energies.

These sources belong to different classes of objects, either Galactic, such as pulsars, pulsar wind nebulae (PWNe), supernova remnants (SNRs), compact binary systems, etc., or extragalactic, such as active galactic nuclei (AGNs) and γ-ray bursts, in which the emission of high energy photons can be produced by different mechanisms. All these results are deeply modifying our understanding of the "non-thermal Universe". The field is extremely dynamic: the observations continuously provide

Received 2 December 2021; Accepted 3 December 2021; Published online 13 January 2021

* Supported by Key Research and Development Project (2018YFA0404204, 2016YFA0400804), the National Natural Science Foundation of China (11905043, 11803011, 12173018, 12121003, 11773014, 11633007, U1931204, U1731136), the Original Innovation Program of the Chinese Academy of Sciences (E085021002), Guangdong Major Project of Basic and Applied Basic Research (2019B030302001) and science research grant from the China Manned Space Project (CMS-CSST-2021-B09)

† E-mail: xiaozhang@nju.edu.cn
‡ E-mail: ygchen@nju.edu.cn
★ Editors ¶ Contributors. All authors contribute equally to the work.

new results, often unexpected and surprising, while the theory makes efforts to clarify the structure of these sources and the mechanisms operating in the acceleration regions.

In this scenario a strong interest is addressed to the development of new instruments capable of making more precise observations, with a better sensitivity and in a more extended energy range. This interest is brought to new ambitious projects, like CTA (Cherenkov Telescope Array [1]), HAWC (High Altitude Water Cherenkov [2]), HiSCORE (Hundred Square-km Cosmic Origin Explorer [3]), and LHAASO (Large High Altitude Air Shower Observatory).

Most results of TeV Gamma Ray Astronomy have been obtained with Imaging Atmospheric Cherenkov Telescopes (IACTs), directional instruments with a field of view (FOV) limited to a few square degrees, that can make observations only in clear and moonless nights. These are obvious limitations in a field of research aimed to discover unknown sources, and where most of objects have variable emissions, in some case explosive and unpredictable as γ-ray bursts, whose emission can last only a few tens of seconds.

Air shower detectors, detecting the secondary particles of γ-ray induced showers reaching the ground, do not have these limitations, since they can continuously observe the whole overhead sky. Air shower detectors like MILAGRO and ARGO-YBJ, even if with a lower sensitivity with respect to Cherenkov telescopes, have obtained relevant achievements. Starting from their results, new instruments based on the same concepts, but with a much higher sensitivity, like HAWC and LHAASO, have been designed to complement in a natural way the observation of future IACTs.

As pointed out before, the fundamental idea of LHAASO is the development of an instrument capable of measuring the cosmic ray (CR) spectrum, composition, and anisotropy in a wide energy range ($\sim$1–10^5 TeV) and at the same time to be a sensitive γ-ray telescope at energies from $\sim$300 GeV to 1 PeV. In particular, the LHAASO design makes the detector particularly competitive in the γ-ray energy range above a few tens of TeVs, an energy region almost completely unexplored. Only a few sources have been observed to emit photons at these energies, and the data are affected by large uncertainties since the sensitivity of current instruments is not enough to determine clearly the spectral shape.

Actually, γ-ray astronomy at and above 100 TeV is of extreme importance since it is related to one of the most puzzling aspects of high-energy astrophysics: the identification of CR sources. Presently there is a general consensus that CRs with energy up to the so-called "*knee*" of the spectrum (2–4 PeV), and probably even up to 10–100 PeV, are accelerated inside our Galaxy. SNRs are long since believed the most likely sources, because the shock wave of the expanding shell could provide the conditions suitable to accelerate particles to relativistic energies, and secondly, the frequency of supernova explosions and their energy release could provide the total energy budget of CRs in the Galaxy [4].

This idea, however, is still lacking clear experimental evidence. Actually TeV γ-rays have been observed from a number of SNRs, demonstrating that in SNRs some kind of acceleration occurs. However, the question whether TeV γ-rays are produced by the decay of π^0 from protons or nuclei interactions, or by a population of relativistic electrons via inverse Compton (IC) scattering or bremsstrahlung, still needs a conclusive answer.

AGILE and Fermi observed GeV photons from two mid-aged SNRs (W44 and IC443) showing the typical spectrum feature around 1 GeV (the so called "π^0 bump", due to the decay of π^0) related to hadronic interactions [5]. This important measurement however does not demonstrate the capability of SNRs to accelerate CRs up to the *knee* and above. A key observation would be the detection of γ-rays of energy as high as a factor 10 – 30 times less than the maximum energy of Galactic CRs. The observation of a γ-ray power law spectrum with no break up to 100 TeV would be a sufficient condition to prove the hadronic nature of the interaction, since the IC scattering at these energies is strongly suppressed by the Klein-Nishina effect.

Recently IceCube reported a first piece of evidence of neutrinos of astrophysical origin of energy 0.4 – 1 PeV [6]. The nature of such a flux has been the subject of intense discussions and different hypotheses have been expressed about the Galactic or extra-galactic origin of the signal. If neutrinos were extra-galactic the γ-rays generated by the same processes would be absorbed by the Cosmic microwave background (CMB) through pair production and would not be observable at Earth, but in case of a Galactic origin of a fraction of the measured neutrino flux, it would be important to detect a photon signal of comparable energy.

LHAASO, thanks to the large area of the array KM2A and the high capability of background rejection, can reach sensitivities above 30 TeV about 100 times higher than those of current instruments, offering the possibility to monitor for the first time the γ-ray sky up to PeV energies.

A. LHAASO sensitivity to gamma-rays

LHAASO can study γ-ray sources over almost 4 orders of magnitude of energy. Figure 1 shows the differential sensitivity in one year measurement, obtained by simulating the response of the detector to γ-ray flux from a source like the Crab nebula one. In the same figure the Crab nebula spectrum is also shown as a reference flux. The LHAASO sensitivity curve is the combination of two components, the first relative to the water Cherenkov de-

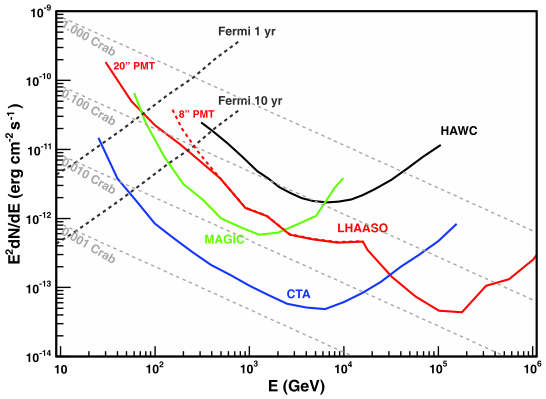

Fig. 1. (color online) Differential sensitivity (multiplied by E^2) of LHAASO to a Crab-like point γ-ray source compared to other experiments. The Crab nebula data obtained by different detectors [8] are taken into account, and the spectral index of 2.6 is extrapolated and extended to 1 PeV.

tector (WCDA), operating in the energy range ~0.3 – 10 TeV, the second relative to the KM2A array, sensitive to energies above 10 TeV [7].

According to simulations, the minimum γ-ray flux detectable by LHAASO is less than 3% of the Crab flux in the energy range ~1-5 TeV and about 10% Crab around 100 TeV. In Fig. 1 the sensitivity curves of other detectors (some in operation, some in project) are also reported. It has to be noted, however, that for a general convention the sensitivity of air shower detectors is reported for one year of operation, while that of Cherenkov telescopes is relative to 50 hours of "on source" measurement. Note that EAS arrays observe every day all the sources in the FOV for a fixed time interval depending on the source declination, while IACTs observe only one source at the time, and only in the season of the year when the source culminates during night time.

The differences in observation times for which the sensitivity curves are evaluated makes the comparison of different detectors not so straightforward. To evaluate the effective performance of different instruments, one must first determine the type of the observation to be done (sky survey, single source follow-up, observation of a flare/burst, etc.). In the observation of a single source during a flare, for example, lasting a certain number of hours, one must consider the sensitivity curves for that observation time. This correction however is not simply obtained by shifting the curves by an amount proportional to the square root of time, because some energy regions can be background free. Due to the different background regime, the sensitivity curves can change shape with different observation time. Decreasing (increasing) the time with respect to the time used in the figure, the background also decreases (increases) and the measurement can be background free at a lower (higher) energy.

Actually, the two techniques - Cherenkov Telescopes and EAS array - are complementary, each of them exploring different aspects of the γ-ray emission. Below 10 TeV, observing a single source, a telescope array as CTA has a higher sensitivity compared to EAS arrays like HAWC and LHAASO. Thanks to the better angular and energy resolution, a Cherenkov telescope can study more in detail the source morphology and spectral features. EAS arrays however have the possibility to monitor a source all days of the year, that in case of AGNs or variable sources in general, it's a clear advantage. Moreover, thanks to the large FOV, they have a much bigger chance to catch unpredictable transient events like flares.

Concerning LHAASO-WCDA and HAWC, their geographical positions (China and Mexico, respectively) allow the observation of the same source at different times during the day, increasing the covering time.

At higher energies LHAASO-KM2A is clearly the most sensitive instrument. According to Fig. 1, at 30 TeV the LHAASO sensitivity is comparable to that of CTA-South and 4 times better than that of CTA-North. Above this energy the sensitivity rapidly increases. The minimum observable flux at 100 TeV is $\sim 3\times10^{-18}$ photons s^{-1} cm^{-2} TeV^{-1}, about a factor ~13 (65) lower than that of CTA-South (CTA-North).

At 1 PeV the minimum flux is $\sim 10^{-19}$ photons s^{-1} cm^{-2} TeV^{-1}. At the same energy, the combined air shower/neutrino detector Ice-Top/Ice-Cube, located at the South Pole, reports a minimum observable γ-ray flux ranging from $\sim 10^{-19}$ to 10^{-17} photons s^{-1} cm^{-2} TeV^{-1} (depending on the source declination) for sources on the Galactic plane in 5 years of measurements [9]. It has to be noted, however, that at these energies the observations can be seriously hampered by pair production with the CMB photons, that can affect the fluxes of Galactic sources with a distance larger than a few kpc.

Using proton and γ fluxes from the Crab direction (with the zenith within 8° ~ 45° and assuming a spectrum index 2.7), the simulated efficiency of γs and protons that pass the hadron rejection cuts is shown on Fig. 2. The simulation includes the ED, MD, and WCDA components of LHAASO. Above 10 TeV the measurement of the μ component in the showers allows a very efficient rejection of CR showers. According to simulations the fraction of CRs that survive the discrimination cuts is 0.01% and 0.004 % at 10 and 30 TeV, respectively, while above ~150 TeV, it is found to be less than 0.0001%. This means that above ~150 TeV the study of the γ-ray emission from a point source can be considered as background free, because after applying the rejection procedure the expected background in a cone around a source is less than one event in one year. The flux has been evaluated by dividing each energy decade into 4 bins, and requiring a statistical significance of 5 standard deviations per bin and a minimum number of 10 events. In the background free regime, only the later constraint is adopted.

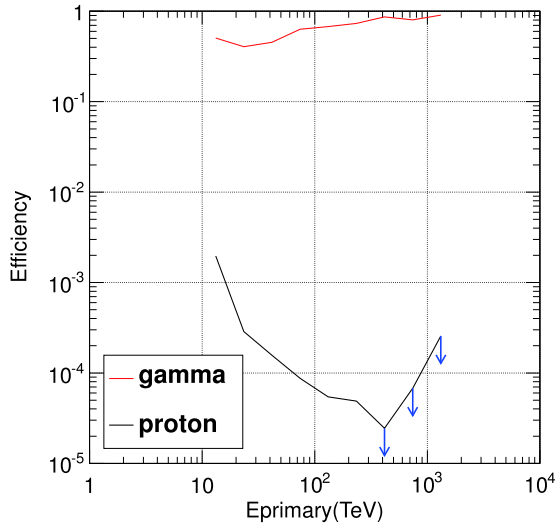

Fig. 2. (color online) Simulated LHAASO detection efficiency of γs and protons: the number of events normalized to a year of flux from the Crab.

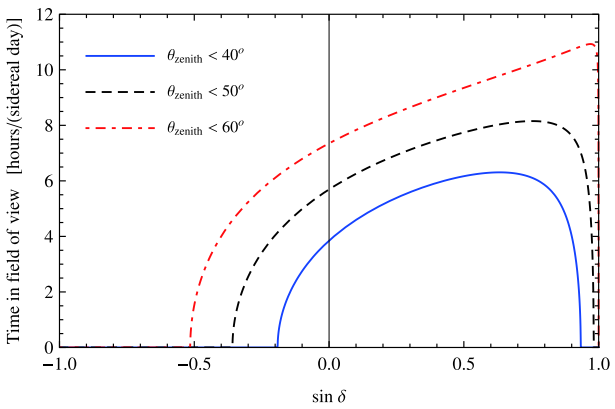

Fig. 3. (color online) Observation time (hours) per day as a function of the source declination, for 3 values of the maximum zenith angle. The area under the curves is proportional to the total exposure (observation time × solid angle).

One should note that in the background free regime, the sensitivity increases linearly with the observation time instead of the square root of time, as in presence of background, and the energy threshold for the background free regime changes with the observation time.

B. LHAASO and sky survey

One of the most interesting aspects of LHAASO is the large FOV and the capability to monitor every day a consistent fraction of the sky. In principle the FOV can include all the sky above the horizon, but the sensitivity decreases at large zenith angles.

Considering only the region of the sky that culminates at zenith angles smaller than 40°, every day LHAASO (located at latitude 29° North) can survey the declination band from −11° to +69° (about 56% of the whole sky) that includes the Galactic plane in the longitude interval from +20° to +225°. Most of this region will be observed by LHAASO with unprecedented sensitivity. For the most energetic events, the extension of the FOV to larger zenith angles will increase the sky coverage allowing observations close to the Galactic center. Fig. 3 shows the observation time per day as a function of the source declination, for different values of the maximum zenith angle.

In the past, the air shower detectors ARGO-YBJ and Milagro have surveyed about the same region of the sky visible by LHAASO, at energies above 0.3-1 TeV and ∼10 TeV respectively, with a sensitivity of about 0.3 Crab units [10, 11]. The new EAS array HAWC, in full operation since 2015, has a sensitivity ∼4 times lower than that expected for LHAASO in the 1–10 TeV region, but more than 100 times lower at 100 TeV. Concerning Cherenkov telescopes, their limited FOV and duty cycle prevent a survey of large regions of the sky. In the past, a fraction of the Galactic plane have been surveyed by IACTs with an excellent sensitivity in the TeV energy range. H.E.S.S. performed a survey of the Galactic plane between longitude −110° and 65° in the latitude band ±3.5° with a sensitivity of ∼0.02 Crab units at energies above 100 GeV [12], which led to the discovery of more than 60 sources, while VERITAS surveyed the Cygnus region between longitude 67° and 82° with a sensitivity of about 0.04 Crab units [13].

It is interesting to compare the performance in sky survey of LHAASO and the future array CTA. Let us consider a survey of the Galactic plane in a longitude interval of 200° and a latitude band from −4° to +4°. A detector like CTA, with its limited FOV, must scan the whole region with different pointings. The number of pointings determines the maximum observation time that can be dedicated to any location. Assuming a FOV of 5° radius and a decrease of sensitivity of about 50% at a distance of 3° from the center (according to the design of SSTs, the CTA-South small area telescopes planned to work at the highest energies), a reasonable step for pointings could be 4°. With this step, 100 pointings are necessary to cover the entire region. Since in one year a Cherenkov telescope can make observations for a total time of ∼1300 hours (assuming the use of the silicon photomultipliers that allow the data taking also in presence of the Moon), every source can be observed for ∼13 hours. At 1 TeV, the CTA-South sensitivity in 13 hours is still higher than that of LHAASO in one year. At ∼25 TeV LHAASO starts to become more sensitive than CTA. Above 30 TeV, the CTA-South sensitivity is no more limited by the background but by the number of detected events (that must be at least equal to 10), hence it must be rescaled linearly with the time. According to this rough estimation, LHAASO would be ∼4 and 50 times more sensitive than CTA-South at 30 and 100 TeV, respectively.

The LHAASO performance is more impressive in case of an all sky survey, where assuming a region of 7 steradians to be scanned, the number of CTA pointings would be as large as ∼1600 and every location would be observed for less than one hour. In this case the LHAASO sensitivity would be more then ∼60 and 800 times higher than that of CTA-South for energies of 30 and 100 TeV, respectively.

Finally, in the comparison with CTA-North (that will be located in the Canary island of La Palma at about the same latitude of LHAASO and will observe about the same sky), LHAASO will gain a further factor 4-5 due to the lower sensitivity of the Northern array with respect to the Southern one. Furthermore, it has to be noted that the CTA-North telescopes will have a FOV with a radius no larger than 4° and consequently the number of pointings necessary to cover the region to be scanned will be larger by at least 40% with respect to the value used above, decreasing correspondingly the observation time and the sensitivity.

C. Galactic gamma-ray astronomy

According to the online TeV source catalogue TeVCat [14] at the time of writing the number of known sources is 169. Among them, 60% belong to our Galaxy and 40% are extragalactic (mostly AGNs of blazar type). About 1/3 of Galactic sources are still unidentified, 1/3 are PWNe, and the remaining are SNRs, compact binary systems and massive star clusters. Note that the sensitivity of the current instruments allows the detection of three "Galactic" sources actually inside an extragalactic object, the Large Magellanic Cloud.

The sky map in Fig. 4 shows the position of all the sources in Galactic coordinates. The sky region that culminates at zenith angle smaller than 40°, delimited by green lines in the figure, includes 84 objects, 23 Galactic, 47 extragalactic, and 14 still unidentified. All the unidentified sources but one lay on the Galactic plane, being probably Galactic objects that cannot be identified due to the number of possible associations in their positional error box.

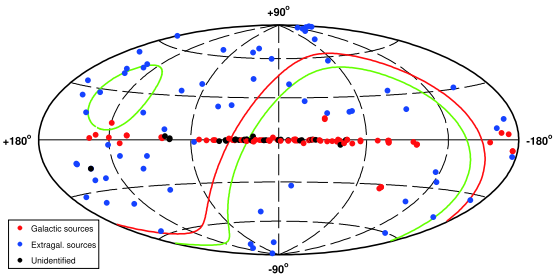

Fig. 4. (color online) Sky map in Galactic coordinates, showing the positions of the known TeV sources. The red line represents the celestial equator. The green lines limits the region of the sky that culminates at zenith angles smaller than 40° at the LHAASO site. The sources are indicated by different colors according to their type: Galactic, extragalactic, unidentified (note that the three sources denoted as "Galactic" around the position RA = 83° and Dec = –69° are actually in the Large Magellanic Cloud).

The spectra of the Galactic sources have been generally measured in the energy range from a few hundreds GeV to 10–20 TeV, and for most of them they are consistent with a power-law behavior. The precise measurement at higher energies would be of extreme interest to understand the emission mechanisms of γ-rays, which for most of the sources are still not understood, and will surely help in the source identification.

So far, only six sources have data above 30 TeV. They are all Galactic and are among the most luminous objects of the TeV sky: the SNR RX J1713.7-3946, the PWNe Crab and Vela-X, and the three MILAGRO extended sources MGRO J2031+41, MGRO J2019+37 (actually resolved in two different sources by VERITAS), and MGRO J1908+06, all of them probably being PWNe, too. Their spectra above 30 TeV are however known with large uncertainties.

PWNe are the most common type of Galactic sources. They are believed to be the product of the ultra-relativistic $e^{\pm}$ wind emitted by young pulsars with large spin-down rates, interacting with magnetic and radiation fields around the pulsar. Other leptons can also be accelerated in the shock produced in the collision of the wind with the environment matter. All these relativistic leptons produce synchrotron and IC radiation.

The Crab nebula, the most luminous TeV source and the first to be detected at TeV energies at the beginning of the Cherenkov telescopes era in 1989, is the most famous example of this class of objects. Its spectral energy distribution (SED) shows a double-humped structure. The first one, extending from radio waves to ∼1 GeV, is due to synchrotron emission, and the second one, peaking at ∼100 GeV, is the product of IC scattering of electrons off low energy photons (synchrotron, thermal, and CMB photons). The SED is well defined up to 10–20 TeV and above this energy is not precisely known. Figure 5 shows the high energy Crab spectrum measured by different ground based experiments [15-19]. Even considering the large error bars, a disagreement is evident among the higher energy data. The HEGRA spectrum is a power law with a weak steepening above 10 TeV whereas MAGIC and H.E.S.S. measurements show a more evident spectral curvature in all the energy range considered. The precise measurement of the high energy emission, the "end" of the spectrum, would bring important information on the particle acceleration and the magnetic and radiation fields in the pulsar environment, constraining some parameters that the lower energy spectrum alone cannot determine unambiguously.

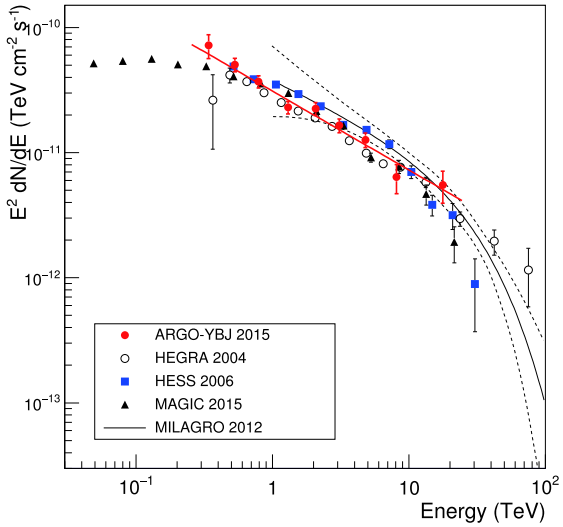

Fig. 5. (color online) Energy spectrum of the Crab nebula measured by different experiments.

The high energy measurement would also be of great importance in understanding the intriguing phenomena of the Crab nebula flares. Since long considered as the "standard candle" for γ-ray astronomy, the Crab nebula has unexpectedly shown a variable behavior in the 100 MeV – 1 GeV energy range, with strong flares lasting hours/days [20-22], and rate variations on time scales of months [23], which are still waiting for a shared interpretation. During flares, the SED shows a new hard component above 100 MeV, generally interpreted as synchrotron emission of a new population of electrons accelerated to energy up to 10^{15} eV, whose origin is still not understood. A TeV flux enhancement in coincidence with the GeV flares have been reported by ARGO-YBJ [24], but with low statistical significance, and has not been confirmed by later measurements by the more sensitive Cherenkov experiments [25, 26]. The question of the possible existence of an IC emission associated to the GeV flares remains open, in particular in the energy region around and above 100 TeV, where the IC emission is more likely to occur. LHAASO is the most suitable detector for such a study, due to the high sensitivity at these energies and to the possibility of observing the Crab nebula for 5–6 hours every day of the year.

Besides the Crab nebula, LHAASO can perform accurate spectral measurements above 30 TeV for most of the known TeV Galactic sources visible from its location. To give a quantitative idea of the LHAASO capabilities, it is useful to compare the detector sensitivity with the fluxes of such sources.

Out of 84 sources crossing the detector FOV with a zenith angle less than 40°, 23 are associated with known Galactic objects, while 13, even if not yet associated with certitude with a source, lay on the Galactic plane, and can be reasonably considered Galactic too. For 35 out of these 36 Galactic sources, the fluxes have been measured and reported in [14] and for 24 of them, spectral indices are available, ranging from 1.75 to 3.1, with an average value of 2.4.

Figure 6 shows the spectra of 35 objects extrapolated to 1 PeV (with the same spectral index measured in the TeV region) compared to the LHAASO one-year sensitivity. The spectral index has been set to 2.5 for the sources without an available spectral measurement. It should be specified that for a correct comparison the LHAASO sensitivity should be calculated for each source using its individual spectrum, angular extension, and declination, while in the figure the sensitivity refers to a Crab-like source. The spectral extrapolations are clearly unrealistic, since the real spectra would likely show steepening or cutoffs at some energies, but the purpose of the figure is to show that the fluxes of almost all the considered sources are above the LHAASO sensitivity. LHAASO can study in detail the behavior of the higher energy emission of most of the sources, down to fluxes of $\sim 3\times10^{-18}$ photons s^{-1} cm^{-2} TeV^{-1}, at 100 TeV in one year of measurement. These high energy data are likely to play a crucial role for the understanding of the properties of the sources.

Among Galactic sources, shell SNRs are probably the most interesting to be studied at high energy because the detection of an emission above 100 TeV could be the footprint of hadronic acceleration. In general, from an emission of hadronic origin, one expects a γ-ray spectrum showing the "π^0 bump" followed by a power law with a slope consistent with parent spectrum slope up to 50–100 TeV, or even more, depending on the parent nuc-

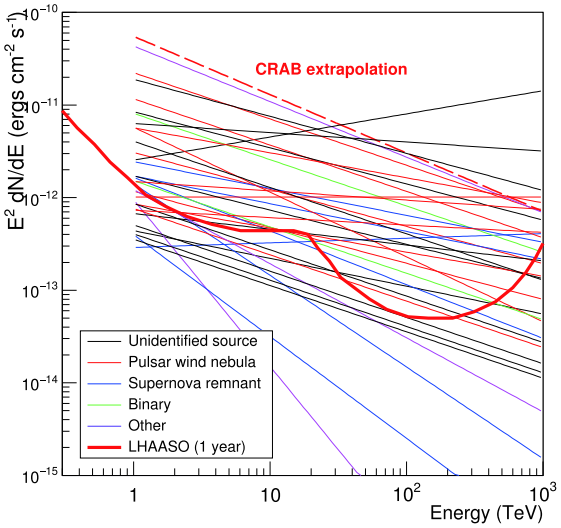

Fig. 6. (color online) Differential spectra (multiplied by E^2) of the TeV γ-ray sources visible by LHAASO extrapolated to 1 PeV, compared to the LHAASO sensitivity. The dashed red line represents the Crab nebula flux, as measured by ARGO-YBJ [15] extrapolated to 1 PeV as a power law.

lei's maximum energy. A leptonic emission (IC scattering of electrons with a power law spectrum) would produce a flatter power law γ-ray spectrum, but with a gradual steepening due to the Klein-Nishina effect. The position of the break depends on the energy of the target photons. For example, electrons with a spectral index of 2.2, scattering off CMB photons, would produce a γ-ray spectrum of index 1.6 in the Thomson regime, that gradually steepens up to 3.2 in the Klein Nishina regime. At 100 TeV the flux is already suppressed by a factor of 3 with respect to the extrapolation of the spectrum before the break.

Actually, in a SNR one could expect a combination of the two emissions, leptonic and hadronic, with different weights depending on many parameters, such as the density of target material for hadronic interaction, the magnetic field strength, the age of the supernova, etc., which make it difficult to identify the emission origin. However, the observation of a spectrum extending above 100 TeV would be a strong indication of a hadronic emission.

So far, only one remnant, SNR RX J1713.7-3946, has been detected above 30 TeV (actually, the spectrum reaches almost 100 TeV [27]). In this case the spectrum steepens above a few TeV and does not show the "π^0 bump", being more consistent with a leptonic emission [28]. All other TeV SNRs have data up to 15 TeV at maximum. Based on the new data, RX J0852.0-4622 [29], Cas A [30], and RCW 86 [31] have a high-energy cutoff around a few TeV.

In the LHAASO FOV there are six shell SNRs (Tycho [32], Cas A [33], W51 [34], IC443 [35], W49B [36], and G106.3+2.7 [37]). The measured spectra show a power law behavior without any cutoff up to the maximum energy reached by the current instruments, that ranges from ~2 to 15 TeV for the sources considered. It should be noted that a recent result of VERITAS [38] shows an updated spectrum of Tycho, steeper than the one reported in the figure, which would make the LHAASO measurement more challenging for this source.

Besides the observation of known sources, given the LHAASO capabilities in sky survey, new Galactic sources will likely be discovered at high energy, since objects with fluxes at 1 TeV below the current instruments sensitivity but with hard spectra (i.e. spectral index <2) would be easily detectable by LHAASO above ~10 TeV.

II. SUPERNOVA REMNANTS

A. Gamma-ray observation of SNRs

Among Galactic γ-ray point sources, SNRs are considered to be one of the most plausible candidates for acceleration of CRs up to PeV energies [41-43]. According to Dave Green's Galactic SNR catalogue[1)], 295 SNRs have been detected up to now. Most of these SNRs are only detected in low energy bands [44]. In the GeV energy range, the Fermi-LAT collaboration reported their first SNR catalog based on three year's survey data, in which 12 firm identifications and 11 possible associations with SNRs were found [40]. In the TeV energies range, there have been at least 23 SNRs or SNR candidates detected up to now, 10 of which are also GeV γ-ray emitters[2)]. Furthermore, there are 34 unidentified TeV γ-ray sources which do not have clear counterparts in other wavelengths. Unlike the Fermi unidentified sources, which are expected to be dominantly constituted by AGNs [45], most of the unidentified TeV sources are located in the Galactic plane (see Fig. 1) and could be potential SNRs. Figure 7 illustrates the locations of those sources (symbol) and their visibility by LHAASO (shaded region). In total, 92 out of 295 SNRs in Green Catalog, 6 GeV SNRs or SNR candidates, 2 TeV SNRs and 6 GeV-TeV SNRs are in the FOV of LHAASO. Moreover, 17 TeV unidentified sources locate in the FOV of LHAASO.

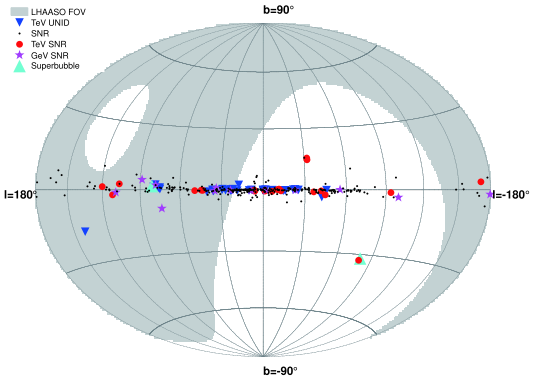

Fig. 7. (color online) Locations of SNRs and unidentified TeV γ-ray sources in Galactic coordinates, compared with the FOV of LHAASO (grey region) [39]. Black dots represent SNRs from Green[1)], red filled circles and magenta stars show TeV[2)] and GeV γ-ray SNRs [40], blue triangles represent the unidentified TeV γ-ray sources, and cyan triangles represent two super-bubbles which were detected in TeV γ-ray bands.

Moreover, it has been found that some SNRs could emit TeV γ-rays while in GeV energy band there was no detection, such as G106.3+2.7 and HESS J1912+101. G106.3+2.7 was first observed by DRAO at radio energy range [46]. In 2000, Pineault & Joncas confirmed the object as an SNR, with an estimated age of 1.3 Myr and distance of 12 kpc [47]. The pulsar PSR J2229+6114 is located at the northern edge of the remnant's head and it is associated with boomerang-shaped radio and X-ray emitting wind nebula. At GeV energy band, the EGRET

1) http://www.mrao.cam.ac.uk/surveys/snrs/
2) http://tevcat.uchicago.edu/

source 3EG J2227+6122 is compatible with the pulsar position, as well as the main bulk of the radio remnant [48]. At TeV energy band, VERITAS reported the total flux from the SNR G106.3+2.7 above 1 TeV is about ~5% of the Crab Nebula in 2009 [37]. HESS J1912+101 is plausibly associated with the PSR J1913+1011, which is detected by H.E.S.S. experiment. The integral flux between 1–10 TeV is 10% of the Crab Nebula and the measured energy spectrum can be described by a power-law with a photon index ~ 2.7. From the current observations on these two TeV SNRs, we can conclude that LHAASO might detect a number of SNRs compared to conservative predictions based on the current SNR catalogs.

B. Hadronic or leptonic origin of the gamma-ray emission

Generally, there are two types of scenarios for the production of high-energy γ-rays from SNRs: the leptonic interaction via IC scattering of background photos by relativistic electrons and hadronic interaction via decay of neutral pions produced by inelastic collisions of relativistic ions with ions in the background plasma [49-52].

Up to now, the evidence for efficient leptonic acceleration in SNRs is clearly established [53, 54]; however, the question whether SNRs are efficient hadron accelerators is more difficult to answer. The recent observations of γ-ray spectra for W44 and IC443 by Fermi show signatures of accelerated protons and nuclei via hadronic interactions with ambient gas and subsequent π^0 decays into γ-rays [5, 55]. But at TeV band, the current observations [35, 56, 57] are not enough to identify the radiation mechanism. With the wide FOV, LHAASO is suitable not only to measure their SEDs but also carry out morphological investigations on those sources at high energies.

Young SNRs, typified by Tycho and Cas A, are believed to be energetic accelerators of relativistic particles. Tycho's SNR, which appeared in 1572 [58], has been observed from radio to TeV γ-ray band [32, 59-64]. At the GeV range, Fermi-LAT reported a 5σ detection of GeV γ-ray emission from Tycho, which can be described by a power-law with a photon index 2.3 ± 0.2 [65]. At the TeV range, VERITAS found that the total flux of Tycho above 1 TeV is ~ 0.9% of Crab Nebula and the spectral index between 1 TeV and 10 TeV is about 1.95 ± 0.51 in 2011. But in 2015, the spectral index turns to 2.92 ± 0.42 [38]. If the spectral index is about 2 up to 10 TeV as VERITAS reported in 2011, it implies that the corresponding spectrum of primary protons extends without a significant steepening or a cutoff to at least several hundred TeV [4, 66]. Due to the large uncertainties of the data sets of Fermi and VERITAS, the energy spectrum from GeV to TeV can be described by a broad range of function, which is not enough to constrain the origin of high energy γ-ray emission.

Cas A, which might appear in 1680, is the youngest of the historical Galactic SNRs [55, 67]. It is one of the best studied objects with both thermal and non-thermal broad-band emission ranging from radio wavelengths to TeV γ-rays [33, 67-69]. TeV γ-ray observations revealed a rather modest γ-ray flux, compared to the synchrotron radio through X-ray emission, which further strengthens the argument for a rather high magnetic field. In the GeV range, Fermi-LAT observation suggests that leptonic model can not fit the turnover well at low energy because the bremsstrahlung component that is dominant over IC below 1 GeV has a steep spectrum, and hadronic emission describing the γ-ray spectrum with a broken power-law is preferred. However, because the observed TeV γ-ray fluxes have large statistical uncertainties, it can not be judged yet whether the TeV γ-rays are generated by interactions of accelerated protons and nuclei with the ambient gas or by electrons through bremsstrahlung and IC scattering. And the maximum energy of the observed TeV γ-rays is only several TeV, the question whether Cas A accelerates particles to PeV energy is still open.

At the LHAASO site, the effective observation time is 6.2 hours per day for Tycho and 6.8 hours per day for Cas A with zenith angle less than 45°. Tycho culminates with a zenith angle of 34° and Cas A culminates with a zenith angle of 29°. The expected spectrum of Cas A from 0.3 TeV to 1 PeV is shown in Fig. 8, in which we can see that from 300 GeV to 500 TeV, the statistic error of data obtained by LHAASO will be less than 10%. Due to the Klein-Nishina effect, the spectrum dominated by electrons is much softer than the hadronic emission above 10 TeV, and the expected result of LHAASO with a low statistic errors can give a reasonable explanation on the high energy range. These estimations show that the LHAASO observation would be just sufficient not only to give the final judgement for the hadronic/leptonic models but also to confirm whether the historical SNRs are PeVatrons or not.

Middle-aged SNRs that are associated with γ-ray emission are usually in interaction with molecular clouds and feature hadronic emission in γ-rays. As one of the well studied middle-aged SNRs, IC 443 possesses strong molecular line emission regions that makes it a case for an SNR interacting with molecular clouds. The X-ray emission of IC 443 is primarily thermal and peaked towards the interior of the northeast shell, indicating that IC 443 is a thermal composite or mixed-morphology SNR. Fermi [70] in the GeV band and VERITAS [35], and MAGIC [71] in the TeV band detected the γ-ray emission from IC 443 and obtained the spectra up to 1 TeV, but there is not yet observation at higher energies, which is very important for determination on γ-ray emission mechanism.

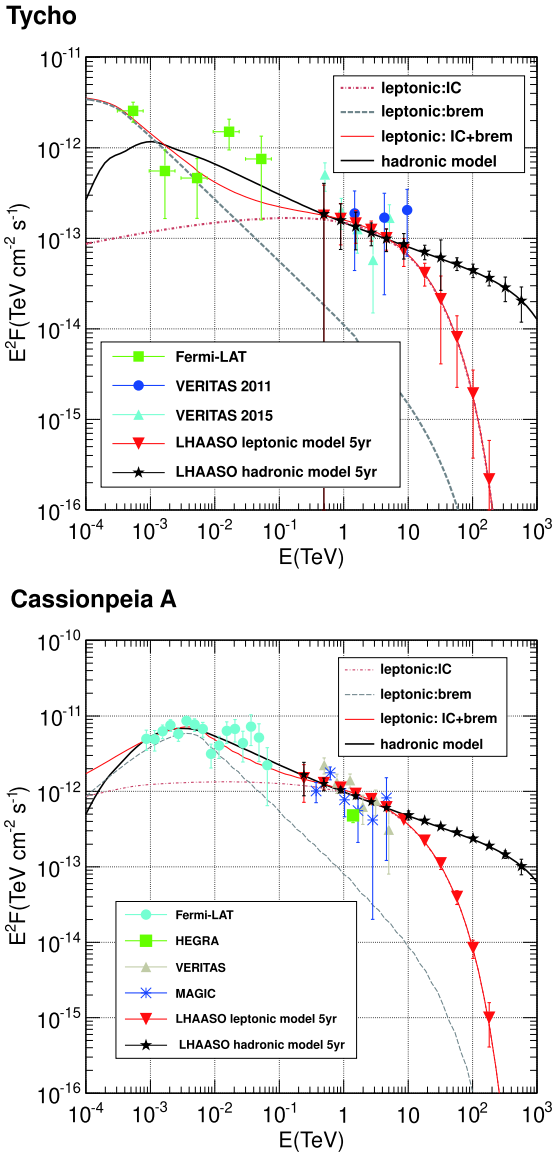

Fig. 8. (color online) Spectral expectation of the LHAASO project on the historical SNRs [39].

The middle-aged SNR W51C (G49.2-0.7) also interacts with molecular clouds. The W51 region was heavily studied as it is known to host several objects. It contains three main components: two star-forming regions W51A and W51B surrounded by very giant molecular cloud, and SNR W51C. W51C is a radio-bright SNR at a distance of 6 kpc from Earth with an estimated age of $\sim 3 \times 10^4$ yr [72]. A smaller distance of 4.3 kpc is also suggested based on the HI absorption results [73], which is supported by the simulation of the radio morphology [74]. W51C is visible in X-rays showing both a shell type and center filled morphology. Shocked atomic and molecular gases have been observed, providing direct evidence on the interaction of W51C shock with a large molecular cloud [34, 75]. The GeV spectral result provided by Fermi indicates that leptonic model is difficult to explain γ-rays production and the most reasonable explanation is that hadronic interaction taking place at the shocked shell of W51C emits GeV γ-rays [76]. Moreover, MAGIC and H.E.S.S. also indicates the γ-ray emission from W51C tends to be dominated by π^0-decay up to several TeV [34, 75, 77]. But this still has uncertainties for studying the acceleration mechanism above 10 TeV.

At the LHAASO site, the effective observation time is 6.53 hours per day for IC 443 and 6.0 hours per day for W51C with zenith angle less than 45°. IC 443 culminates with a zenith angle of 8° and W51C culminates with a zenith angle of 16°. The expectation of LHAASO is given in Fig. 9, compared with the measurement of Fermi, MAGIC and VERITAS. From 300 GeV to 500 TeV, the statistic error of data obtained by LHAASO will be less than 10%. The discrepancy between the expectations

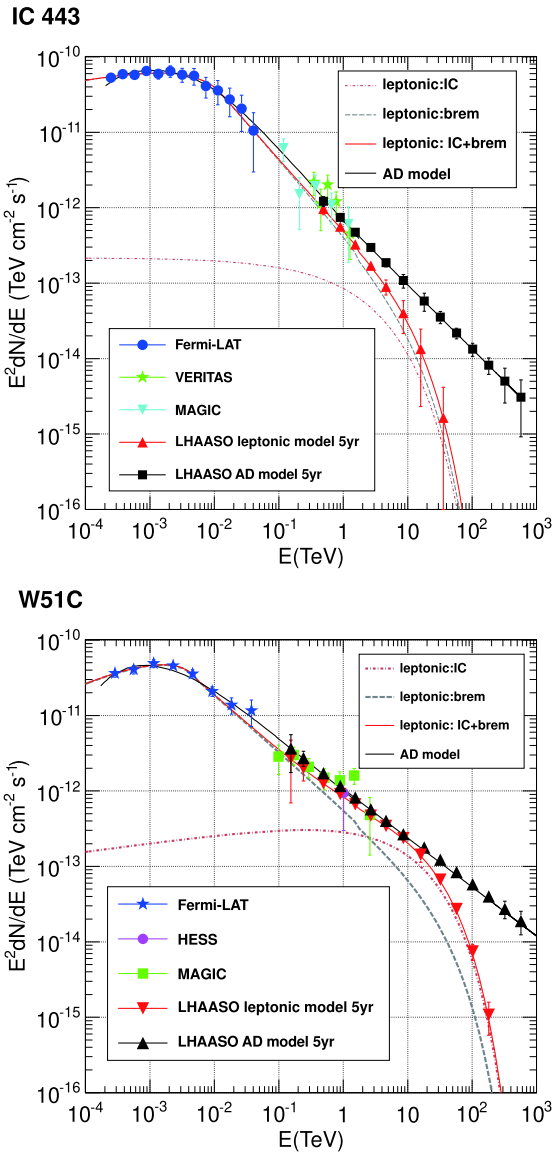

Fig. 9. (color online) Spectral expectation of the LHAASO project on SNRs' interaction with molecular clouds [39].

from the two models will reach more than 5 sigma above 20 TeV. It indicates that LHAASO will make a great contribution to the acceleration measurement in the TeV range, providing the final judgement on leptonic or hadronic origin.

C. Are SNRs PeVatrons?

LHAASO will be powerful in showing whether Galactic SNRs are PeVatrons or not. Whether young SNRs are PeVatrons or nor may have an effect on their γ-ray spectra. With 158h of high quality data, MAGIC collaboration [30] updated the TeV γ-ray spectrum of SNR Cas A and revealed a high-energy cutoff of 3.5 TeV with 4.6σ significance. This spectral feature seems to rule out Cas A as a PeV particle accelerator if the TeV γ-ray emission has a hadronic origin. However, the cutoff also can be explained by the leptonic process in a two-zone model [78]. In this model, the electrons accelerated by the forward shock (zone 1) dominantly contribute the TeV γ-rays via the IC process, while the GeV γ-rays are mainly produced by the protons accelerated by the inward/reverse shock (zone 2) (see Fig. 10). Thus, the proton spectrum does not need a cutoff, implying that Cas A could still be treated as a PeVatron. Moreover, the hadronic γ-rays from zone 1 can dominate the hundreds of TeV range if the total energy in the relativistic protons accelerated by the forward shock reaches the order of 10^{48} erg, which is also sufficient to supply the high-energy component of CR ions in the frame of SNR origin of Galactic CRs [79]. This two-zone model also could be applied to the Tycho SNR and explain the very soft TeV spectrum observed by VERITAS (see the top panel of Fig. 10). The spectral data obtained with LHAASO can thus be used to determine the maximum energy to that energetic protons can be accelerated by the SNR shock wave.

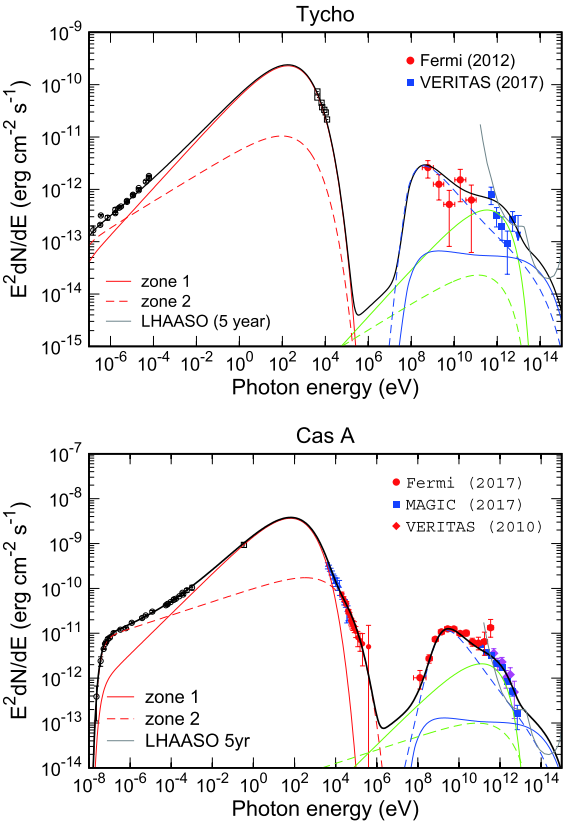

Fig. 10. (color online) SED of SNR Cas A and Tycho. The black solid line represents the total emission from zone1 (solid) and zone 2 (dashed) with components: synchrotron (red), IC (green), and *p-p* collision (blue).

Using the hadronic interaction model for the diffusive protons [51, 52], Fig. 11 shows the expected hadronic spectra of the middle-aged SNRs W28, W41, W51C, and CTB37A for a proton energy cutoff at 3PeV, which are within the detection ability at the TeV photon energy for 5-yr LHAASO observation.

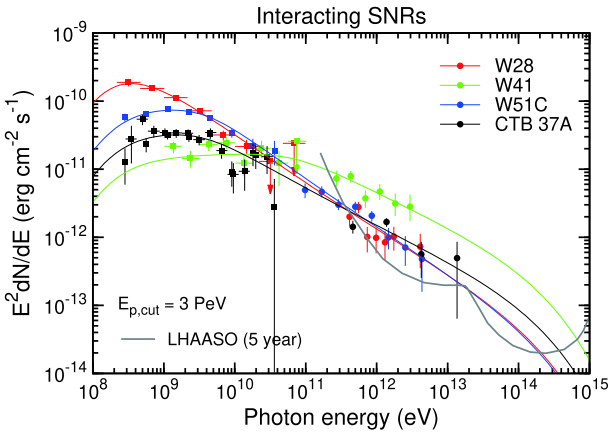

Fig. 11. (color online) Hadronic emission spectra expected for four SNRs that interact with molecular clouds using the diffusive proton model [51, 52].

III. STAR-FORMING REGIONS

Star-forming regions are the factories of stars, containing young OB stars and related super-bubbles with strong collective stellar winds. The wind shocks and turbulence created by the collective stellar winds can accelerate particles to the relativistic regime. So they are the potential CR sources. On the one hand, the recent measurements of ^{60}Fe abundance in CRs [80] indicate that a substantial fraction of CRs could be accelerated in young OB star clusters and related super-bubbles. Furthermore, the measurements of the Galactic diffuse γ-ray emission show that the CRs have a similar radial distribution as OB stars rather than SNRs [81, 82]. On the other hand, super-bubbles do have sufficient kinetic energy, supplied by supernova explosions therein or collective stellar winds, to provide the flux of the locally measured CRs [83]. Meanwhile, theses objects should be visible in γ-

rays due to the freshly accelerated CRs interacting with ambient gas. In this regard a principal question is whether these objects can operate also as PeVatrons, i.e. whether they can provide the bulk of the locally observed CRs up to the so-called *knee* around 1 PeV. The most straightforward and unambiguous answer to this question would be the detection of γ-rays with a hard energy spectrum extending to energies well beyond 10 TeV.

A. Cygnus region

The Cygnus region of the Galactic plane is the famous region in the northern sky for the complex features observed in radio, infrared, X-rays, and γ-rays. It contains a high density interstellar medium and is rich in potential CR acceleration sites such as Wolf-Rayet stars, OB associations, and SNRs. This region is home of a number of GeV γ-ray sources detected by Fermi-LAT [84] and several noteworthy TeV γ-ray sources detected by Milagro and ARGO-YBJ in the past decade. The Cygnus Cocoon, located in the star-forming region of Cygnus X, is interpreted as a cocoon of freshly accelerated CRs related to the Cygnus super-bubble. The extended TeV γ-ray source ARGO J2031+4157 (or MGRO J2031+41) is positionally consistent with the Cygnus Cocoon discovered by Fermi-LAT at GeV energies in the Cygnus super-bubble, and another TeV source MGRO J2019+37 is a mysterious source only being detected by MILAGRO [85, 86] above 20 TeV and VERITAS [13] above 1 TeV. The reason for the hard SED from such a spatially extended region is totally unknown. The discovery of this kind of sources and the more detailed multi-wavelength spectroscopic investigations can be an efficient way to explain the radiation mechanism of them.

Figure 12 shows all the spectral measurements by Fermi-LAT [87], ARGO-YBJ [88], Milagro [86], and the expectation results with LHAASO. One year observation of LHAASO will be sufficient to give a judgement on the different energy cutoff models from 300 GeV to several hundred TeV. It will provide important information for investigating the particle acceleration within the super-bubble.

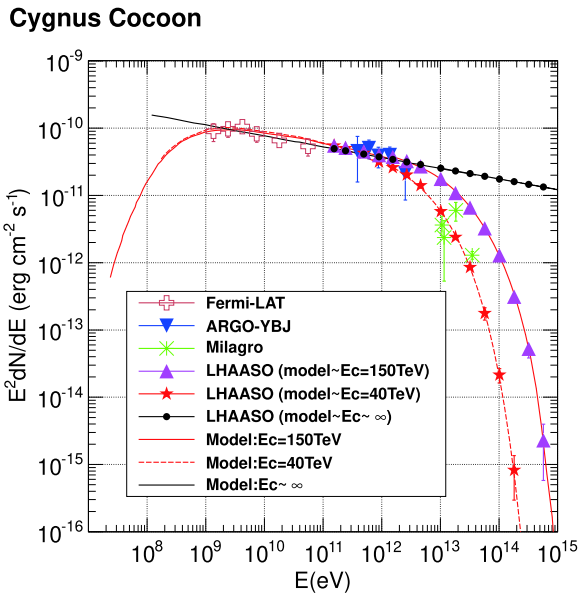

Fig. 12. (color online) Expectation of the LHAASO project on Cygnus Cocoon by using one year MC data [39], compared with the measurement of Fermi-LAT [87], ARGO-YBJ [88], Milagro[85, 86].

B. W49A: a Galactic mini-starburst

As a part of the W49 complex [89], the powerful thermal radio continuum source W49A is one of the brightest Galactic giant radio H II regions ($\sim 10^7 L_\odot$) and is identified as an active star-forming region. It is located in a giant molecular cloud with a total mass of $\sim 10^6 M_\odot$ [90, 91] and is the best Galactic analog to the starburst phenomenon seen in other galaxies. This region contains ~ 40 ultracompact H II regions, each hosting at least one massive star (earlier than B3) [92], and the brightest water maser cluster in our Galaxy [93]. Based on the proper motion of the strong H_2O masers, the distance is estimated to be 11.4 ± 1.2 kpc [94]. These massive stars can output a copious amount of kinetic energy via stellar winds, which may be sufficient to accelerated CRs. Two expanding shells as well as remnants of two gas ejections were found in W49A [95]. The shells may be driven by the massive stars and have a total kinetic energy of $\sim 10^{49}$ ergs. The gas ejections are likely to have the same origin as the expanding shells and a total energy of $\sim 10^{50}$ ergs. All these observational results make it as a likely potential γ-ray source. Indeed, the observations of H.E.S.S. telescopes toward the direction of W49A reveal an excess of TeV γ-rays with a significance of more than 4.4σ [36], although the GeV emission has not been reported.

However, another star-forming region NGC 3603 was detected by Fermi-LAT as an extended source with radius of 1.1° at a significance level of more than $\sim 10\sigma$ [96]. Although NGC 3603 is not located in the FOV of LHAASO, its properties in the GeV band may give some clues to explore the TeV γ-rays for the other star-forming regions. The spectrum of NGC 3603 in energy range from 1 to 250 GeV didn't show any sign of cutoff and can be well fitted with a single power law with a photon index ≈ 2.3, indicating the existence of the particles with multi-TeV energies at least. In Fig. 13, the Fermi-LAT data are modeled via the hadronic scenario with different proton cutoff energy. As can be seen, LHAASO observation toward the other star-forming regions, including W49A, may help us to answer whether energetic particles can be accelerated up to PeV in the star-forming regions.

Further consideration of LHAASO targets of candidate PeVatrons harbored in star forming regions will be given in Sec. VII.C.

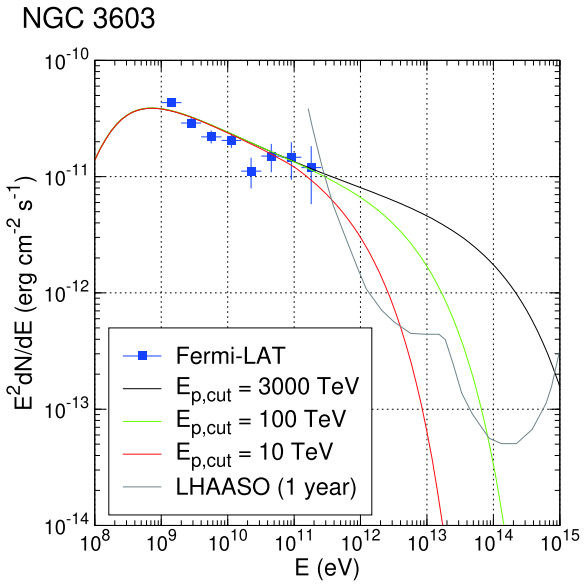

Fig. 13. (color online) Modeling the Fermi-LAT data of source NGC 3603 [36] with the different proton cutoff energies: 3000 TeV (black), 100 TeV (green) and 10 TeV (red), compared with the LHAASO's sensitivity curve (gray).

IV. PULSARS AND PULSAR WIND NEBULAE

A. High-energy TeV emission from pulsars

Thanks to Fermi Gamma-ray Space Telescope, which was launched in 2008 June, we have learned from its observations that pulsars are the dominant γ-ray $0.1-100$ GeV sources in our Galaxy [40]. Thus far more than 200 pulsars have been detected by Fermi, and from the studies we now know that pulsars generally have γ-ray emission described by a power law with exponential cutoff at several GeV. Such a spectral shape matches the theoretical expectations, as the emission arises due to curvature radiation from the magnetosphere (near the magnetic poles) of a pulsar (e.g., [97]). It was certainly a surprise when 100 GeV pulsed emission from the Crab pulsar was detected by VERITAS [98], and recently the MAGIC Collaboration has recorded the photons with energies up to 1.5 TeV [99]. In addition, pulsed photons above 50 GeV from the Vela pulsar were also detected [100]. Is such high energy emission only seen from the brightest, young pulsars? Not really! In a recent paper, [101] has reported the detection of up to 200 GeV photons from an old, so-called millisecond pulsar (MSP; they spin rapidly, at periods of several milliseconds).

The detection of photons above 100 GeV challenges the theoretical understanding of the pulsar emission mechanisms, because all the pulsar emission models predict a cutoff in the curvature radiation of pulsars as large as $\sim$100 GeV. Currently the IC scattering process in the outer magnetosphere or the pulsar wind region is considered to produce the pulsed emission detected in the ≥ 10 GeV band from the Crab pulsar (see, e.g., [102, 103]). Alternatively, a non-stationary outer-gap scenario has also been proposed recently [104], in which the observed spectrum of a pulsar is the superposition of emission from the variable outer gap structures.

LHAASO will certainly explore the high-energy TeV emission from pulsars, helping by finding a full sample of them and setting constraints for theoretical modeling. We note that high-energy γ-ray emission is seen from 27 pulsars, as reported in the first Fermi catalog of sources above 10 GeV [105]. Among them 20 sources were found to have pulsed γ-ray emission in the >10 GeV band, including 17 young pulsars and three MSPs. Such sources in the FOV could be good targets for LHAASO.

B. Pulsar wind nebulae

Pulsars are powered by their fast rotation, and most of the rotational energy of a pulsar is released in a form of the pulsar wind (see, e.g., [106]). The high-energy, relativistic particles in the pulsar wind interact with the ambient medium around a pulsar forming a terminal wind shock. Particles at the shock emanate synchrotron radiation, making the PWN bright from radio to X-ray energies. At GeV and TeV γ-ray energies, it is believed that the IC scattering process gives rise to emission, with electrons of Lorentz factor $\sim 10^6$ up-scattering background infrared photons to GeV/TeV range. The modeling of a broad-band spectrum of a PWN thus allows us to study its particle population, magnetic field, and dynamical evolution (after the birth of the pulsar; e.g., [107-109]). Especially, when a PWN enters the last evolutionary stage in which the pulsar escaped from its parent SNR or its parent SNR almost disappeared, the original PWN will first dim in the low energy band, leaving an extended TeV emission region called "TeV halo"[1)] [110-112] (see Sec. IV.C for more details). Thus far, more than 30 PWNe or candidates have been detected at TeV energies, and Fermi has been able to detect a few of them [113]. Particularly, the first astrophysical source detected above 100 TeV is the prototype PWN Crab, which was achieved by the Tibet AS+MD [114] and HAWC [115] experiments. More recently, HAWC collaboration released a $\geq$56 TeV catalog [116] containing nine sources which all are likely related to pulsars and may be TeV halos. With LHAASO's great sensitivity around 100 TeV and large-sky area monitoring capability, it is conceivable that more PWNe or halos will be detected, allowing to obtain a full sample of them in the northern sky.

Apart from SNRs, PWNe are also believed to be a kind of Galactic CR source. According to the Hillas criteria [117], the particles with energy below the *knee* en-

1) It was called "TeV PWN" in the early literature.

ergy can be effectively trapped by the magnetic fields of PWNe. Thus, PWNe could store a large amount of energy in relativistic protons if pulsars or PWNe could continuously produce energetic protons. Based on the outer magnetospheric gap model, Cheng *et al*. [118] pointed out that the Crab pulsar can produce relativistic protons if $\vec{\Omega}\cdot\vec{\mu}>0$, where $\vec{\Omega}$ and $\vec{\mu}$ are the angular velocity and magnetic moment of the star, respectively. It is recently suggested that the PWNe inside SNRs can further accelerate the relativistic protons that were accelerated by the SNR shocks up to an energy of order 1 PeV, and hence such PWNe may also be PeVatrons [119]. If a PWN is located in a dense environment and contains relativistic protons, the hadronic emission from the energetic protons may have a significant contribution to the GeV-TeV γ-rays [120]. Indeed, the lepton-hadronic model has been applied to some PWNe to explain their broadband spectra, e.g. in the cases of Vela X [121], G54.1+0.3 [122], DA 495 [123], and G106.3+2.7 [124, 125]. Of course, it is also pointed out that protons can only take away the spin-down energy of pulsars with a very small fraction [126, 127]. With LHAASO's great capacity of detecting γ-rays up to energy of ~ 100 TeV, it may help us testing the proton acceleration in PWNe.

Space experiments (PAMELA [131], Fermi [132], AMS-02 [133]) have revealed an excess of high-energy positrons relative to the standard predictions for secondary production in the interstellar medium (ISM). In order to explain this positron excess, it can be confirmed that significant quantities of TeV positrons should be produced within the local volume (the surrounding ~ kpc), but the source of positrons is still in debates. Pulsars and/or PWNe are widely suggested to be the dominant sources of the local population of TeV electrons and positrons, which can account for the observed positron excess [134-138]. Among the known pulsars, Geminga (PSR J0633+1746) and B0656+14 (PSR J0659+1414) are the potential sources due to their short distance to us. These two pulsars are relatively young (370 and 110 kyrs, respectively) and are located within a few hundred parsecs of the solar system (250^{+230}_{-80} and 280^{+30}_{-30} pc, respectively [139]). The electrons and positrons released by the pulsars can diffuse into the surrounding medium and produce γ-rays. Indeed, the extended TeV γ-ray emission ($2^\circ-3^\circ$ radius) surrounding the Geminga pulsar, a prototype TeV halo, has been reported by Milagro [128] and HAWC [129], although the observations by the MAGIC telescopes[1)] show no significant detection above 50 GeV [130]. The extended TeV γ-ray emission from B0656+14 also has been detected by HAWC [129]. Based on the HAWC results, Hooper et al. [138] calculate the expected contributions from the two pulsars to the local positron spectrum via fitting the γ-ray spectrum and conclude that pulsars are likely sources of the local TeV positrons. In Fig. 14, the observed results for Geminga and the LHAASO's sensitivity are shown. As can be seen, LHAASO has the ability to accurately measure the γ-ray spectrum from 200 GeV to 100 TeV, which will give more stronger constraints on the properties of these pulsars and test the pulsar scenario of the positron excess, thus settling the dispute between the MAGIC and HAWC observations.

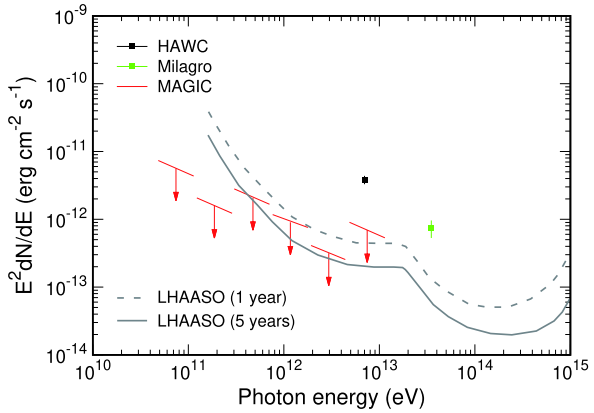

Fig. 14. (color online) The spectrum of the nebula around the Geminga pulsar measured by Milagro [128], HAWC [129] and MAGIC [130].

C. TeV gamma-ray halos

In continuation of the above discussion of TeV halos, more specific issues are detailed here.

1. *Very slow-diffusion halos around pulsars*

In late 2017, the HAWC collaboration reported the spatially resolved measurement of the γ-ray halos around the Geminga pulsar and PSR B0656+14 (Fig. 15) [129]. Unlike γ-ray PWNe, which are confined structures around young pulsars. These two γ-ray halos should be generated by free electrons and positrons ($e^{\pm}$s) diffusing out from the corresponding PWNe. The Geminga pulsar and PSR B0656+14 are middle-aged pulsars (0.1–1 Myr). According to the evolution model of PWNe [106], the original PWNe of these pulsars were already broken long time ago, and now these pulsars are traveling in the ISM, driving bow-shock PWNe with scales much smaller than the TeV halos. This is consistent with the X-ray observations [140, 141]. In the ISM, the observed multi-TeV γ-rays are mainly emitted by $e^{\pm}$s through IC scattering of the homogeneous CMB, so the γ-ray spatial profile should unambiguously indicate the diffusion speed of the escaping $e^{\pm}$s. This may be so far the most straightfor-

1) It is difficult for IACTs to detect the large extended sources.

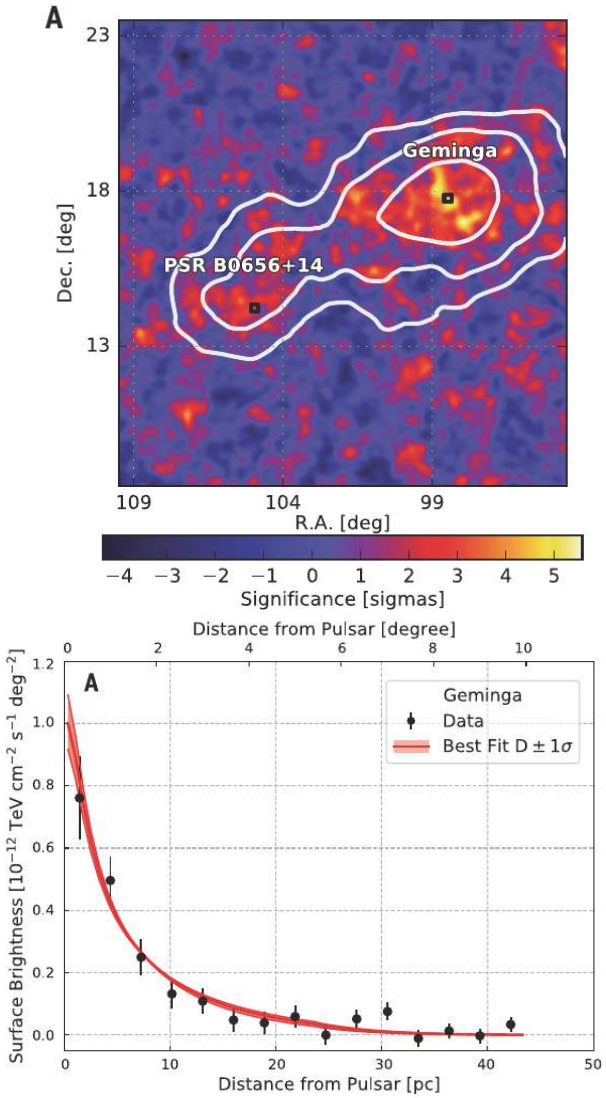

Fig. 15. (color online) Top: HAWC significance map for the region around Geminga and PSR B0656+14. Bottom: surface brightness profile around Geminga. Both adopted from [129].

ward measurement of CR propagation in local regions of the ISM.

However, the diffusion coefficient derived from these halos is several hundred times smaller than that indicated by the CR boron to carbon ratio (B/C) [142]. The latter is currently the most important indicator of the global CR propagation in the Galaxy. With the diffusion coefficient derived from B/C, the CR antiproton spectrum and the Galatic diffuse γ-rays can be well reproduced (e.g. [143]). Thus, the slow diffusion around the two pulsars must not be representative in the whole Galaxy. Then what picture would it be? Does the slow diffusion only happen in the nearby region of pulsars? Or is it common in the Galactic disk? The answer of this question could be vital for investigating the origin of CRs, for example, the origin of the positron excess.

Geminga and PSR B0656+14 are generally believed to be the most likely sources of the positron excess [134, 136, 144], due to their close ranges and the capability of accelerating high-energy $e^{\pm}$s. However, if the slow diffusion is everywhere in the local environment of the solar system, positrons released by these pulsars can hardly arrive at Earth [129]. In this case, a very close pulsar is required to explain the positron excess [145-147]. In contrast, if the slow-diffusion regions are only limited in the vicinity of the pulsars, Geminga may still be a probable source of the positron excess [138], and even more optimistic than in the former fast-diffusion case [148].

There are also efforts in studying the possible origin of the slow-diffusion halos. The most straightfoward explanation may be the self-generated case, in which the slow diffusion is induced by the escaping $e^{\pm}$s from the pulsars through streaming instability [149]. While considering the proper motion of Geminga [150], the slow-diffusion halo must be a newly formed structure. The injection power in the recent age of Geminga is too small to significantly suppress the diffusion coefficient [151]. In contrast to the self-generated scenario, the slow diffusion region could be preexisting [151]. If the progenitor of Geminga was in a rarefied environment, the current scale of the associated SNR of Geminga could be large enough to include the Geminga pulsar and the TeV halo inside. Although the SNR is too old to be visible at present, it could be energetic enough to leave a turbulent environment for Geminga, which explains the slow diffusion. Besides, it is also possible that the TeV halos are not interpreted by a turbulent environment, but by the anisotropic diffusion of $e^{\pm}$s along the local regular magnetic field lines which are required to be aligned with the line of sight towards the pulsars [152]. All these interpretations should be tested by a larger sample of TeV halos.

2. *Significance of TeV-halo observation*

Currently, new TeV halos around pulsars (such as PSR J0633+0632 and PSR B0540+23) are detected by HAWC with high significance [153]. TeV halos are thus very likely to be common around middle-aged pulsars. Observation of this type of sources has significant meanings:

• As mentioned in Sec.IV.C.1, TeV halos around middle-aged pulsars are ideal tools for studying the CR propagation. Firstly, the background level in the energy range of multi-TeV is much lower than that in low-energy γ-ray observations. This helps us to obtain clear γ-ray profiles around sources, which carry the information of particle propagation. Secondly, the observed TeV γ-rays are generated by very young $e^{\pm}$s. For example, 20 TeV γ-rays are emitted by $\sim$ 100 TeV $e^{\pm}$s, the lifetime of which is only $\sim$ 7 kyr. Thus, the γ-ray spatial distribu-

tions unambiguously indicate the present MHD status of the ISM around the pulsars. This means an evolution-independent model is enough to explain the data, in which we do not need to consider some complicated factors like the proper motion of the pulsars and the evolution of the ISM. Thirdly, compared with young SNRs, middle-aged pulsars should be better targets for the study of CR propagation. For the latter, the high-energy $e^{\pm}$s are accelerated by pulsars or PWNe, the sizes of which are significantly smaller than those of the TeV halos. So the propagation zone will not be mixed with the acceleration zone, and a clear pattern of CR propagation can be obtained.

• TeV halos could be indicators for invisible pulsars [110]. Pulsars are lighthouse-like emitters. We cannot detect the pulsed signal from pulsars if their electromagnetic emission is not beamed towards Earth. In this case, extended TeV halos could be implications for those misaligned pulsars. This is especially meaningful for relatively old pulsars whose host SNRs already faded. Follow-up observations in multiwavelengths would then provide further evidence about the origin of the halos.

• We can derive the $e^{\pm}$ injection spectra from the observation of TeV halos. The injection spectra include the information of particle acceleration and escaping in PWNe. Current observations show that even relatively old sources like Geminga can still accelerate particles to at least ~ 100 TeV. Energy spectra of more halos will be measured in the future, which may reveal the relationship between the acceleration limit of PWNe and other parameters, such as the ages of the pulsars.

3. *Candidate Objects for LHAASO*

With its high sensitivity, wide energy range, and large FOV, LHAASO is very competent to perform deep investigation of TeV halos. In Table 1, we list the top 30 bright middle-aged pulsars in the ATNF catalog [154], which could be the targets of the future observation. Of course, we only choose those within the FOV of LHAASO ($-10° < \mathrm{Dec} < 70°$). The pulsars are ordered by $\dot{E}/r^2$, where $\dot{E}$ is the current spin-down luminosity of the pulsar and r is the distance to the pulsar. Obviously, the two halos reported by HAWC [129] correspond to the two brightest pulsars. The pulsar age t in the table is limited between 50 kyr and 10 Myr. As we mentioned in the beginning, what we focus on here are the halos generated by the free $e^{\pm}$s diffusing in the ISM, rather than the confined PWNe. For pulsars younger than ~ 50 kyr, the original PWNe may not be totally broken, which might be confused with the free diffusion halos. There is also discussion about the criterion of TeV halos [112].

It can be found from the "comment column" of Table 1 that current TeV experiments have already measured the top 10 bright sources. However, γ-ray halos are not significantly detected for three of them—PSR B1951+32, PSR J1740+1000, and PSR J1836+5925. We note that all of these three pulsars are relatively far from the Galactic plane (146 pc for B1951+32,420 pc for J1740+1000, and 126 pc for J1836+5925). In fact, all the pulsars with height larger than 100 pc (from Galactic plane) in Table 1 are not detected with TeV halos so far. Does it imply that the slow-diffusion region is a very thin disk in the Galaxy which is possibly left by myriad old SNRs? Or is the non-detection due to other reasons? The future measurement of LHAASO may give an explanation to it.

V. GAMMA-RAY BINARIES

A new class of high-mass X-ray binaries (HMXBs) have been discovered as strong γ-ray emitters: PSR B1259−63, LS 5039, LS I +61° 303, HESS J0632+057, and 1FGL J1018.6−5856 (see [155] for a review). Other recent candidates such as PSR J2032+4127 have also been reported [156]. These γ-ray binaries contain a compact object orbiting an OB companion star, emitting non-thermal emission from radio to TeV γ-rays that are modulated on the orbital period. Studying the emissions from γ-ray binaries can probe the surroundings of compact objects at AU scale, which is a largely unexplored distance scale. The complexity of the immediate environment of γ-ray binaries also shed light on physical processes that are poorly understood.

The detection of very high energy (VHE) γ-rays (above 100 GeV) by the current IACTs from all known γ-ray binaries, gives hint for very efficient particle acceleration in these systems. Indeed, there is no lack of particle acceleration sites for γ-ray binaries: the interaction of the pulsar wind (for those the compact object is a pulsar) with the strong wind of a massive star, accretion onto a compact object and/or jet activities (similar to micro-quasars), and a relativistic outflow interacting with the ISM at a larger scale. Micro-quasars or interacting stellar binaries are also observed to emit γ-rays above 60 MeV, e.g., in Cygnus X-1 [157], Cygnus X-3 [158], V 404 Cyg [159], and Eta Carinae [160].

γ-ray binaries, such as LS 5039, have a very high efficiency of particle acceleration. The very good sensitivity of LHAASO in the energy band of 10 –100 TeV and above will allow us to probe the acceleration mechanism, the magnetic field strength, stellar wind densities, and short-term variability of the acceleration and/or radiation regions. This is because the opacity and orbital dependence of γ-γ absorption, and the angular dependence of the IC emission, or other sources of variability, are less important in this energy range than in sub-TeV energy band. In addition, the spectrum of the emission also depends on whether the accelerated particles are leptons or hadrons.

Table 1. The top 30 bright middle-aged pulsars within the FOV of LHAASO[a]. The parameters of the pulsars are given by the ATNF catalog.

NAME	RA(°)	Dec(°)	l(°)	b(°)	r (kpc)	t (100 kyr)	$\dot{E}$ (10^{34} erg s^{-1})	$\dot{E}/r^2$ (10^{34} erg s^{-1} kpc^{-2})	Comments
J0633+1746	98.5	17.8	195.1	4.3	0.19	3.42	3.25	90.03	Geminga, detected by HAWC
B0656+14	105.0	14.2	201.1	8.3	0.29	1.11	3.80	45.18	detected by HAWC
B1951+32	298.2	32.9	68.8	2.8	3.00	1.07	374	41.56	with X-ray PWN, missed in TeV
J1954+2836	298.6	28.6	65.2	0.4	1.96	0.69	105	27.33	detected by Milagro
J1740+1000	265.1	10.0	34.0	20.3	1.23	1.14	23.2	15.33	with X-ray PWN, missed by HAWC
J1913+1011	288.3	10.2	44.5	−0.2	4.61	1.69	287	13.50	detected by H.E.S.S.,YBJ,HAWC
J1836+5925	279.1	59.4	88.9	25.0	0.30	18.3	1.14	12.67	missed in TeV
J2032+4127	308.1	41.5	80.2	1.0	1.33	2.01	15.2	8.59	detected in X-ray,TeV
J1928+1746	292.2	17.8	52.9	0.1	4.34	0.83	160	8.49	detected by HAWC?
J1831-0952	277.9	−9.9	21.9	−0.1	3.68	1.28	108	7.97	detected by H.E.S.S.,HAWC
B0114+58	19.4	59.2	126.3	−3.5	1.77	2.75	22.1	7.05	
J0633+0632	98.4	6.5	205.1	−0.9	1.35	0.59	11.9	6.53	detected by HAWC
J0248+6021	42.1	60.4	136.9	0.7	2.00	0.62	21.3	5.33	
B0355+54	59.7	54.2	148.2	0.8	1.00	5.64	4.54	4.54	the Mushroom X-ray PWN
J1938+2213	294.6	22.2	57.9	0.3	3.42	0.62	36.6	3.13	
J0538+2817	84.6	28.3	179.7	−1.7	1.30	6.18	4.94	2.92	X-ray PWN, missed by HAWC?
B1830-08	278.4	−8.5	23.4	0.1	4.50	1.47	58.4	2.88	with X-ray PWN
J2043+2740	310.9	27.7	70.6	−9.2	1.48	12.0	5.64	2.57	
J2021+4026	305.4	40.4	78.2	2.1	2.15	0.77	11.6	2.51	detected in X-ray,TeV
J1857+0143	284.4	1.7	35.2	−0.6	4.57	0.71	45.1	2.16	detected by H.E.S.S.,HAWC
B0611+22	93.6	22.5	188.8	2.4	1.74	0.89	6.24	2.06	
J1841-0345	280.4	−3.8	28.4	0.4	3.78	0.56	26.9	1.88	
J1913+0904	288.3	9.1	43.5	−0.7	3.00	1.47	16.0	1.78	
B0540+23	85.8	23.5	184.4	−3.3	1.56	2.53	4.09	1.68	detected by HAWC
J1846+0919	281.6	9.3	40.7	5.3	1.53	3.60	3.41	1.46	
J0611+1436	92.8	14.6	195.4	−2.0	0.89	10.7	0.80	1.01	
J0357+3205	59.5	32.1	162.8	−16.0	0.83	5.40	0.59	0.85	missed by ASgamma
J1838-0549	279.7	−5.8	26.3	0.2	4.06	1.12	10.1	0.61	
B0919+06	140.6	6.6	225.4	36.4	1.10	4.97	0.68	0.56	
J1835-0944	278.9	−9.7	22.5	−1.0	4.22	5.25	5.64	0.32	

[a] Part of the information is collected from http://snrcat.physics.umanitoba.ca/

LHAASO, being an excellent all-sky detector at the TeV to multi-TeV energies, are a good monitor of the TeV transient sky, including transient phenomena related to γ-ray binaries.

For γ-ray binaries, the most surprising transient behavior came from the GeV observations of PSR B1259-63. During late 2010 to early 2011, the Fermi-LAT observed PSR B1259-63 through a periastron passage, for the first time since its launch in 2008. Before and during the passage, the LAT detected a weak emission above 100 MeV. Unexpectedly, a GeV flare occurred 30 days after the passage, with a flux about an order of magnitude higher than the pre-periastron value. The flare continued about three months after the periastron passage [161, 162]. It turned out that the GeV flare was seen again in 2014 periastron at a similar orbital phase as in 2011. The major obstacle to understand the GeV flare is that it occurred at an orbital phase well after the second/post-periastron disk crossing, and did not correspond to any activities in other wavelengths as of 2011. Although PSR B1259-63, visible only from southern hemisphere, is not visible to LHAASO, this highlights the possibility that any VHE

emission from γ-ray binaries can be unpredictable and transient, which is best probed by an all-sky detector like LHAASO.

In fact, unexpected 'flares' of VHE emission was already seen before. LS I +61° 303 is one of the most studied γ-ray binaries but the nature of its compact object is still under debate because of the poorly constrained mass of the compact object and the inclination angle of the system. Radio to γ-ray emission are all modulated at the orbital period (26.5 days) and even at the super-orbital period of 1667±8 days. VERITAS observations of LS I +61° 303 clearly observed VHE flares in two consecutive orbits in similar orbital phase (October and November 2014; [163]). Figure 16 shows that the 0.3–20 TeV flux of the VHE flare is about a factor of 2–5 above that of the average flux measured previously, and the flare spectrum does not show any cut-off up to 20 TeV. With the planned sensitivity of LHAASO, it is possible that the VHE emission can be seen by LHAASO, if such elevated TeV level remains for months.

Although leptonic scenario prevails to explain the multi-wavelength emissions from γ-ray binaries, if hadrons are also accelerated in the complicated binary environment, they might also contribute to >10 TeV emission. An observational `evidence' for hadronic emission is a low-significance neutrino signal (pre-trial p-value is 0.087) from HESS J0632+057 reported by the IceCube collaboration [164]. Although this signal is fully compatible with the background fluctuation after taking the trial factor into account, if similar events are detected in the future, it could increase the likelihood of a >10 TeV emission from accelerated hadrons.

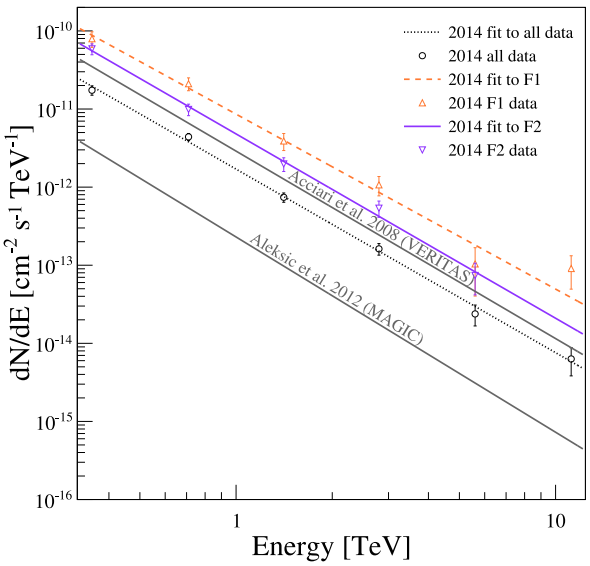

Fig. 16. (color online) Differential spectra of LS I +61° 303 during a flaring period from the VERITAS observations in 2014, together with those average spectra in previous publications (from [163]).

Chances are that there are more γ-ray binaries to be discovered, based on the fact that known γ-ray binaries tend to be nearby. Paredes *et al.* [165] estimate that the total number of γ-ray binaries in our Galaxy is about 50, but this number can depend on the duty cycle of γ-ray emission: VHE emission in HESS J0632+057, LS I +61° 303, and PSR B1259−63 is strongly dependent on orbital phase and in some sources the orbital periods can be (very) long, e.g., the 30–50-year orbital period binary pulsar PSR J2032+4127 has only been recently discovered by long-term monitoring (i.e., years) by the Fermi-LAT. With its very large FOV at all times, LHAASO will be the best instrument to observe known and yet-to-discover γ-ray binaries at energies above 100 GeV.

VI. THE GALACTIC CENTER

A. Galactic center as a high energy emission source

It is well known that the Galactic Center (GC), with a supermassive black hole ($\sim 4\times10^6 M_\odot$), is a good laboratory for the study of high energy astrophysical phenomena. Currently, the overall behavior of the GC is quite silent except some continuous weak activities. Transient X-ray events with a 2–10 keV energy output up to 10^{35}ergs^{-1} are observed from the GC on a regular basis, as well as transient events at MeV/GeV energies. Flares from the X-ray binaries located in the GC region can reach luminosities up to 10^{37}ergs^{-1}. However, there are sufficient evidences to prove that the GC had violent activities in the past, such as X-ray outbursts [166] and the Fermi-Bubbles [167]. During the violent activities, the accretion of stars and gas by the supermassive black hole could be effective to accelerate particles. The maximum energy that protons can achieve by diffusive shock acceleration is [168]

$$E_{\rm max} \sim eBR \approx 10^{14}\left(\frac{B}{\rm G}\right)\left(\frac{R}{10R_g}\right)\ {\rm eV}, \qquad (1)$$

where B is the magnetic field and R is the size of the acceleration region. As in [168], we assume the acceleration takes place within 10 Schwarzschild radii ($R_g \sim 10^{12}$ cm) of the black hole. To accelerate protons to above ~PeV requires magnetic field strength of tens of G in the acceleration region [169, 170]. Such a condition could be reached in the very central region of the GC [168, 171]. On the other hand, if the acceleration takes place in larger regions, the required magnetic field could be smaller. When the accelerated CRs diffuse out of the GC, hadronic interaction with the ISM will happen and produce similar amount of γ-rays and neutrinos. The observations of high energy γ-ray emissions can shed new light on the acceleration mechanism at the GC. In fact, with the state of

art technologies, current γ-ray observations have provided unprecedented sensitivity in studying the acceleration activities in the GC.

B. Gamma-ray emission of the GC

The very high energy γ-rays from hundreds of GeV to tens of TeV in the direction of the GC have been observed by several atmospheric Cherenkov telescopes such as CANGAROO [172], VERITAS [173, 174], H.E.S.S. [175-178], and MAGIC [179]. The diffusive γ-ray emission is also observed at Galactic Center Disk range by H.E.S.S. experiment [176]. More interesting thing is that the map of the central molecular zone as seen in γ-rays demonstrates a strong correlation between the brightness distribution of VHE γ-rays and the locations of massive gas-rich complexes [180]. This points towards a hadronic origin of the diffuse emission, where the γ-rays result from the interactions of relativistic protons with the ambient gas.

Figure 17 shows the spectra of VHE γ-rays for the diffuse emission of GC. The best-fit to the data found that the spectrum with power law index ~2.3 can extend the energies up to tens of TeV, without any indication of a cutoff or a break. It is suggested that such a γ-ray spectrum, arising from hadronic interactions, is detected in general for the first time. Since these γ-rays result from the decay of neutral pions produced by p-p interactions, the derivation of such hard power-law spectrum implies that the spectrum of the parent protons should extend to energies close to 1 PeV. Simultaneously, the spectral index at TeV energy range for the GC point source is the same as that of the diffusive one, which may possibly share the same origin: GC supermassive black hole. The result supports that the γ-ray emissions come from ~PeV energy protons and the most plausible accelerator is the GC [180].

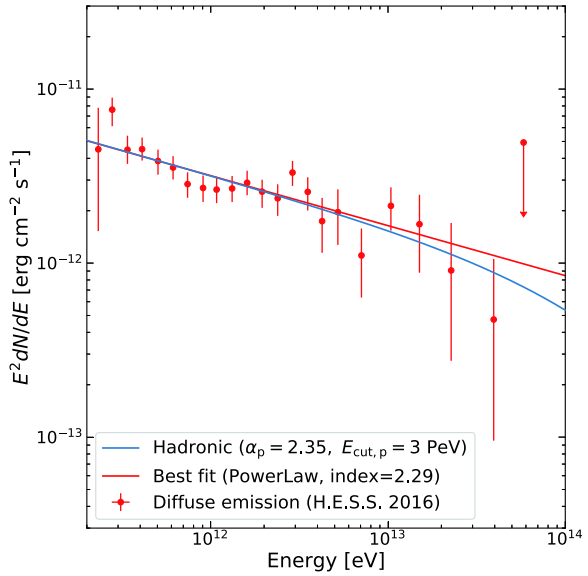

Fig. 17. (color online) The VHE γ -ray spectra for the diffuse emission of GC (Data are adopted from [180]).

However, the γ-ray emission from the point source in GC has a broken power law spectrum at tens of TeV. The best fit of the cut-off can be described by exponential function in high energy [181]. While adopting the traditional model of interstellar radiation field, the absorption effect is too small to explain the observed cut-off spectrum of HESS J1745-290 [181]. The alternative solution attributes it to the intrinsic cut-off, which characterizes the acceleration limit of the flaring event with the critical energy $E_c \sim 200$ TeV for protons. Let us look into the diffuse γ-ray emission at GC region. The uncertainty at tens of TeV in the γ-ray spectrum leads to the poor ability to discriminate the different energy cutoff of protons. It is to say that the observation of γ-ray emission at ~100 TeV energy will play a very important role to determine the acceleration ability of GC in the future.

C. The LHAASO sensitivity at 100 TeV energy range

The problem is that the GC in LHAASO FOV is with the zenith angle of $\sim 65°$, which will seriously reduce the sensitivity of LHAASO. So the special analysis technology for wide FOV should develop to study the γ-ray emission from the GC region based on the simulation. The air shower development in the atmosphere has been generated with the CORSIKA v7.405 code [7]. The electromagnetic interactions are described by the EGS4 package while the hadronic interactions are reproduced by the QGSJET model. The low-energy hadronic interactions are described by the FLUKA package. CR spectra have been simulated in the energy range from 10 TeV to 10 PeV. About 8-yrs showers have been sampled in the zenith angle interval from 55° to 70°. For γ-rays, we produce 20000 events at every energy point including: 50, 100, 200, 500, 1000 TeV. The experimental conditions (trigger logic, time resolution, electronic noises, etc.) have been taken into account via a GEANT4-based fast simulation code and analyzed with the same reconstruction code.

The event selection is performed for the reconstructed simulation data. With the specified cut the backgrounds of CRs can be almost totally rejected. Figure 18 is the effective area of KM2A array. It can reach $\sim 5\times10^3$ m^2 at 50 TeV, $\sim 3\times10^4$ m^2 at 100 TeV and larger than $\sim 2\times10^5$ m^2 above 200 TeV. Owing to the zero background, 10 γ-ray events detected can be defined as 5 σ level. Fig. 19 shows the sensitivity of LHAASO with one year observation. It is obvious that LHAASO have enough sensitivity to observe this source at above 100 TeV. However, if the protons can not be accelerated to ~PeV, LHAASO can not have enough sensitivity.

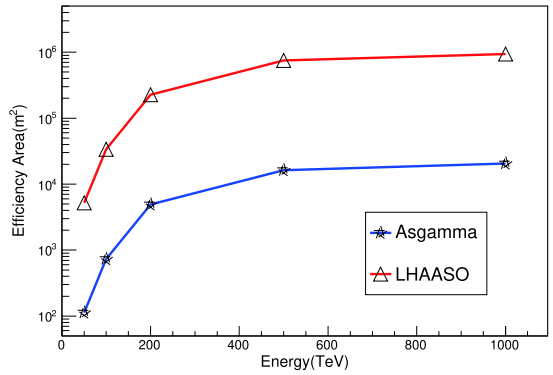

Fig. 18. (color online) The effective area of LHAASO for γ-rays from the GC direction.

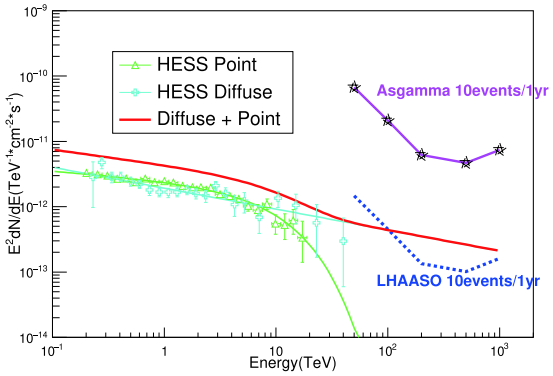

Fig. 19. (color online) The sensitivity of LHAASO for γ-rays from GC direction.

D. Short summary

Galactic CRs can reach energies of $\sim$ PeV. The first PeV accelerator, GC, has been evidenced by H.E.S.S. experiment based on the observation of γ-ray emission at tens of TeV. However, the uncertainty at tens of TeV for the spectrum of γ-rays leads to the poor ability to discriminate the different energy cutoff of protons. We employ the MC simulation to examine the LHAASO sensitivity to Galactic center at 100 TeV energy range and see that LHAASO has enough sensitivity with one year observation to detect this source at above 100 TeV if the protons can be accelerated to PeV energy. On the contrary, if the maximum energy is $\sim$ 200 TeV, LHAASO can not have enough sensitivity to detect it.

VII. GIANT MOLECULAR CLOUDS

A giant molecular cloud (GMC) has a typical mass of 10^5 solar mass and a density of higher than 100 cm^{-3}. The molecular gas in GMCs can be observed and measured via molecular lines, such as the rotational transition lines of CO. Furthermore the infrared emission from the dust inside GMCs provides an alternative way to study the gas contents. GMCs are the birth place of young stars and thus also harbor HII regions and bubble-like structures. GMCs are also regarded as γ-ray emitters. The main γ-ray production mechanisms inside GMCs are the decay of neutral pions produced in the collision of CR nuclei with the ambient gas, IC of relativistic electrons on background radiation fields, and bremsstrahlung of relativistic electrons. Due to the high gas density, pion-decay dominates over the other mechanisms above about 100 MeV [182]. In the energy range of LHAASO, the IC and bremsstrahlung are further suppressed due to the high energy cutoff at several TeV observed in the CR electron spectrum [183]. The dominance of pion-decay mechanism in γ-ray production makes it an ideal place to measure CR density beyond the solar system. Several famous GMCs locate inside the FOV of LHAASO. Their positions, mass, and distances are listed in Table 2. The predicted γ-ray flux from GMCs are proportional to the value M/d^2, which are also listed in Table 2.

A. GMCs as CR calorimeter

The current paradigm of CRs postulates that, because of the effective mixture of CRs during their propagation in the interstellar magnetic fields, the CR density locally measured in the neighborhood of Earth should correctly describe the average density of CRs throughout the Galactic disk [184]. However, small variations of CRs on large (kpc) scales do not exclude significant fluctuations on smaller scales, particularly in the proximity of young CR accelerators. Therefore, it is not obvious that the locally measured component of CRs can be taken as an un-

Table 2. Properties of the GMCs in the FOV of LHAASO. The estimated distance and position are obtained from Dame *et al.* [185]. The mass values listed in the second column are calculated from the CfA maps (see [192] for detail).

Region	M [10^5 $M_\odot$]	D/pc	l (°)	b (°)	M/d^2 [(10^5 $M_\odot$/kpc^2)]	size [arcdeg^2]
ρ Oph	0.12	165	356	+18	8.4	68
Orion B	0.78	500	205	−14	3.9	22
Orion A	1.2	500	213	−18	5.2	28
Mon R2	1.1	830	214	−12	1.7	19
Taurus	0.30	140	170	−16	15.0	101
Polaris flare	0.055	230	130	+26	0.96	40

disputed representative of the whole Galactic population of relativistic particles. In particular, it is possible that the flux of the local CRs might be dominated by the contribution of a few nearby sources. However, the density of CRs in different parts of the Galaxy can be probed uniquely through observations of γ-rays from GMCs [186-188]. On GeV band the investigations in this regard have already been done on the nearby GMCs in Gould belt [189-192] as well as on Sgr B complex in Galactic center [193]. But on TeV band the GMCs are still left undetected. One reason for the non-detection of GMCs is the extended size of these objects and the limited FOV of IACT. In contrast, the high sensitivity and large FOV of LHAASO will provide a unique opportunity to detect such objects and measure the CR density in TeV-PeV band in different positions of the Galaxy. To show the detection prospect we plot the predicted γ-ray flux as well as the LHAASO sensitivities for a typical GMCs with a M/d^2 value of 10^6 ($M_\odot$/kpc^2) in Fig. 20. It should be mentioned that the sensitivities for extended sources are estimated as $F_{\rm ext} = F_{\rm PS}(\Omega_{\rm ext}/\Omega_{\rm PSF})^{1/2}$, where $F_{\rm ext}$ and $F_{\rm PS}$ are sensitivities for the extended source and point source, respectively, and $\Omega_{\rm ext}$ and $\Omega_{\rm PSF}$ are the angular size of extended source and point spread function, respectively. Thus the detection capacity of GMCs depends on their angular size. Indeed, the GMCs show filamentary morphology and the γ-ray emission region is much smaller than that listed in Table 2. Thus the estimation of LHAASO sensitivities in Fig. 20 is very conservative and should be regarded as an upper limit.

In addition to the absolute CR fluxes at different positions of the Galaxy, it would be also possible to measure the spectral property of CRs using the γ-ray observations on GMCs. Recently a hardening in CR spectrum above 200 GeV was reported by several observations [194-196].

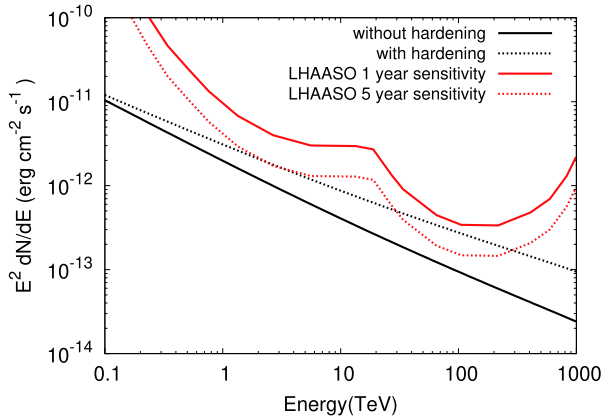

Fig. 20. (color online) The γ-rays flux produced in a molecular clouds with a M/d^2 value of 10^6 ($M_\odot$/kpc^2), the angular size is 20 arcdeg^2. The CR spectrum measured by AMS-02 extrapolated to 10 PeV with and without a hardening are used in deriving the γ-ray flux. The LHAASO sensitivities are estimated by considering the source extension.

This effect can be observed in the γ-ray flux in the nearby GMCs given the hardening extends to more than 100 TeV. To illustrate the effect we plot in Fig. 20 the predicted γ-ray flux in GMCs with and without such a hardening. Furthermore, the γ-rays above 100 TeV are already produced by CRs with the energy close to the *knee*. Thus, LHAASO observation of γ-rays from GMCs in this energy range will provide an alternative method in measuring the CR spectral property near the *knee*.

B. Young stellar associations inside GMCs

Young star associations and corresponding superbubbles are considered to be the origin of a substantial fraction of Galactic CRs [80, 197]. Fermi LAT has detected a cocoon like structure near the young star association of Cygnus OB2 with a hard spectrum and argue that this is produced by fresh accelerated CRs [87]. The GMCs harbor various young star associations and young HII regions. For example, the Orion Nebula Cluster in the Orion A molecular cloud and NGC 2024 in the Orion B molecular cloud are the two largest clusters in the youngest subgroup of Orion OB1, with ages less than 2 Myr [198]. These young star clusters are also potential accelerating sites of the CRs. Although these young accelerators are not observed in GeV band, one can not exclude the possibility that they would dominate in multi-TeV ranges, due to their hard spectra. In this case the CR density inside GMCs are contaminated by the embedded acceleration and GMCs can no longer be regarded as CR calorimeters. Furthermore, if the hard spectra in these young structures are detected in multi-TeV energy range, this would be a strong evidence for the existence of PeVatron, which will be discussed in detail in an independent section (VII.C).

C. PeVatrons

The hard spectrum in multi-TeV range without cutoff is usually considered as the sign of hadronic origin of the emissions. This is because the Klein-Nishina (KN) effects will introduce a break in the spectrum of IC scattering off CMB photons at this energy range, even if there is no cutoff in electron spectrum. Thus such a hard spectrum can only be produced by CRs protons with energy up to PeV. This argument has been adopted for the PeVatrons in Galactic center observed by H.E.S.S. [199] (also see Sec.VI).

As a result, all the hard TeV sources without detected high energy cutoff can be regarded as candidates for PeVatrons. As already discussed in the section "SNRs" (see Sec. II, Sec.II.C), young SNRs might be regarded as PeVatron candidates. Along with young SNRs, the unidentified TeV sources without cutoff should also be examined. One recent example is the H.E.S.S detection of hard spectra up to more than 20 TeV without cutoff in the source HESS J1641-463 [199]. However, the limited statistics

cannot rule out a cutoff at higher energy caused by KN effects. By comparison, the much higher sensitivity of LHAASO at the energy range of 10–100 TeV provides an ideal window to study the spectral property of the PeVatron candidate. Although HESS J1641-463 is located beyond the LHAASO FOV, there are still a few unidentified Galactic sources in the northern sky with hard spectra.

One remarkable example is TeV J2032+4130 in Cygnus region (Sec. III.A), which is also related with the Fermi Cygnus cocoon [87]. The hard spectra (index of 2) and non-detection of cutoff at TeV range has been reported by VERITAS [13]. Furthermore, the study on Fermi Cygnus cocoon reveals that the Cygnus region indeed harbors CR acceleration site and fresh CRs. The Cygnus region, as well as other star-forming regions (see Sec. III), is a very promising target to hunt for PeVatrons.

Another interesting source is HESS J1848-018. H.E.S.S measurement has revealed a spectral index of 2.8 [200], which makes it unlike a PeVatron. However, the recent HAWC observations [201] reveal a much higher flux at high energy and thus a harder spectra. The difference may come from the diffusive nature of this source. The source is spatially correlated with the star forming region W43, which has a similar environment as that of the Cygnus cocoon (Sec. III.A). We note that, at GeV range, the Cygnus cocoon also has a spatial extension of more than 3 degrees. Indeed, if the CRs are accelerated in the super-bubbles surrounding the young star clusters, the γ-ray emission should be diffuse due to the low ambient density in the cavities. Such diffuse structure can hardly be detected by IACT due to the very limited FOV. LHAASO, however, with much larger FOV and continuous exposure, has the capability to detect such structures.

In conclusion, in addition to the strong indication of the Galactic center (Sec. VI), the hard unassociated TeV sources noted here, SNRs (Sec. II), PWNe (Sec. IV.B), and star-forming regions (Sec. III) considered in the previous sections can be Galactic PeVatron candidates. Whether high energy cutoff is present at dozens of TeV is crucial to identify the PeVatron nature of these sources. The energy range of LHAASO is perfectly suitable to study their spectral features. On the other hand, the PeVatrons can also be diffusive rather than compact, and such kind of sources can hardly be detected by the former IACTs but would be very promising to be detected by LHAASO.

VIII. DIFFUSE GALACTIC GAMMA-RAYS

It is recognized that the γ-rays above 100 MeV chiefly spring from the diffuse emission. Three major mechanisms are thought to be responsible for the creation of γ-rays, and they are [202]: the decay of neutral pions which are generated through the inelastic collisions between CRs (mostly protons and heliums) and ISM, the IC scattering of high energy electrons off interstellar radiation field, as well as the bremsstrahlung of CR electrons with interstellar gas. Each process is dominant in different energy bands of the γ-ray spectrum.

Observation of these diffuse emission is beneficial in acquiring the following knowledge: 1) spatial distributions of hadronic and leptonic components of CRs, 2) origin and propagation of CRs in the Galaxy, 3) composition and allocation of interstellar medium, and 4) large-scale distribution of Galactic magnetic field and turbulence. Moreover, as the Galactic diffuse emission often represents the natural background to many different signals, a thorough understanding of diffuse Galactic γ-ray emission (DGE) is also essential for deducing the spectra of other components of the diffuse emission, unveiling the undiscovered γ-ray sources, enhancing the measurement accuracy of the position and SED of Galactic or extragalactic point/extended sources, and even searching for the sign of dark matter annihilation or decay.

A. Progresses on the observations of Galactic diffuse gamma-rays

The observation of diffuse γ-rays started with the OSO-III satellite in 1968 [203]. The measurements have been dramatically ameliorated during the surveys of SAS-2 [204], COS-B [205], COMPTEL [206, 207], HEAO 1 [208] and EGRET [209]. With the launch of a new generation telescope, Fermi, it maps the γ-ray sky up to a few hundreds of GeV with unprecedented accuracy [210, 211], which deepens our understanding of the generation and propagation of Galactic CRs. In lower energies, the SPI instrument on INTEGRAL observatory has extended the observations of CR-induced diffuse emissions into the hard X-ray range [212, 213]. As for the higher energies, subject to very low flux and limited area of space-based detector, the observations above TeV have been carried out principally on ground-based instruments, such as Whipple [214], HEGRA [215], Milagro [85], H.E.S.S. [216], ARGO-YBJ [217] and so on.

Higher-quality data enable us to model the DGE based on CR transport and interactions in magnetic halo [210, 211, 218-220]. In the GeV energy range, the EGRET data show a significant excess in all directions (called "GeV excess") with respect to the predictions supposing the same CR spectrum in the Galaxy as that at Earth. But this excess has not been confirmed by the following observation of Fermi-LAT at intermediate Galactic latitudes [221]. Up to now, the DGE model generated by the numerical package GALPROP well conforms the observations at both high and intermediate latitudes published by the 21-month Fermi-LAT survey [210]. But in the Galactic plane the models all underestimate the data above a few GeV, especially toward the inner Galaxy. This has been reconfirmed in the renewed

measurements by Fermi-LAT [211]. Possible explanations include the contribution from the unresolved point source population such as pulsars, SNRs, PWNe, spectral variations of CRs or even dark matter annihilation/decay [222, 223]. Recently Guo *et al*. [224] suggest that a hard CR component within the Galactic plane can self-consistently explain the excess of diffuse γ-rays at the inner Galaxy and the observed B/C and $\bar{p}/p$ ratios. For the diffuse TeV γ-rays, the Milagro telescope made the first observation towards the Galactic disk and corroborated the existence of diffuse TeV γ-ray emission [225, 227]. In the Galactic plane, the Cygnus region inhabits abundant CR sources and large column density of matter, and is recognized as the brightest γ-ray region in the entire northern sky [226]. Milagro telescope performed the observations of Cygnus region and found the diffuse TeV γ-ray emission [85]. Subsequently ARGO-YBJ experiment carried out similar observation as well [217], whose data agree well with the measurements of Fermi-LAT at lower energies. Meanwhile, H.E.S.S. telescope array also performed surveys at both the Galactic plane [216] and center [176, 180].

Probably, the most spectacular discovery about the extended emission in recent years is the so-called Fermi Bubbles [167, 227]. The Fermi bubbles are two giant lobes, roughly symmetrically distributed at two sides of the Galactic center. Each bubble owns an oval emission region with sharp edge, which extends over several kiloparsecs beyond the Galactic plane. Compared with the diffuse γ-rays, the Fermi bubbles have a visibly harder γ-ray spectrum with index ~ 2, see Fig. 21. So far the origin of Fermi bubbles is still under debate. Many theories have been proposed including jet radiation of massive black hole at the Galactic center, shock wave from accretion events of the central black hole, shock wave from supernova explosions near the Galactic center and so forth (see [228] and references therein).

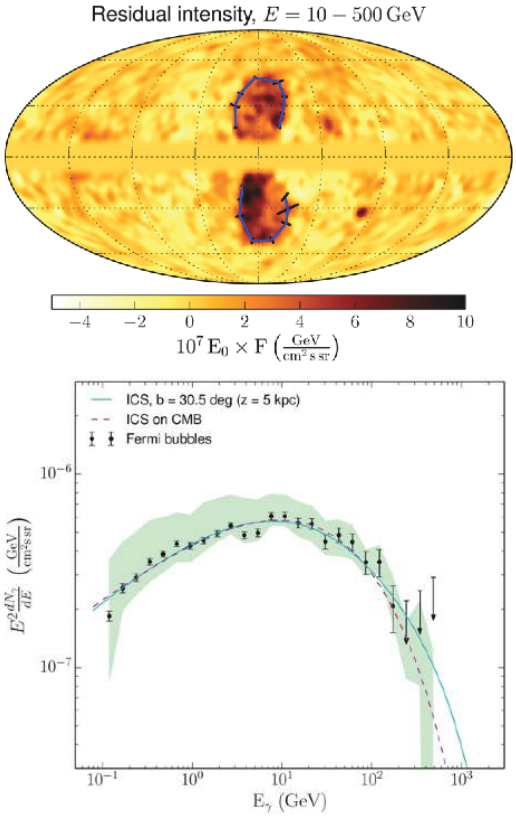

Fig. 21. (color online) Image (top) and SED (bottom) of Fermi bubbles [227].

B. The outlook of LHAASO project on Galactic diffuse gamma-rays above 30 TeV

Nevertheless the above intriguing findings only reach to energies around tens of TeV at most, while for the higher energy, i.e. 100 TeV γ-rays, the observations so far are still poor. One main part of the LHAASO project, KM2A, is designed to observe the γ-rays above 30 TeV. The large detection area and high capability of background rejection enable the sensitivities of LHAASO experiment to reach ~ 100 times higher than that of current instruments above 30 TeV [7, 229]. It will also be the first time to monitor γ-ray sky at PeV energies.

(1) *The observations of diffuse γ-rays above tens of TeV* LHAASO project plans to map the DGE above a few hundreds GeV throughout the Galaxy with high sensitivity. It is going to perform an unbiased sky survey of the northern sky with a detection threshold of ~ 0.03 Crab unit at TeV energies and ~ 0.1 Crab around 100 TeV by one year operation, respectively, which is capable of continuously surveying the γ-ray sky from 100 GeV to 1 PeV. For the LHAASO sensitivity to the DGE flux, it can be evaluated roughly according to the point source sensitivity multiplied by a correction factor $f = (\Omega_{\rm PSF}\Omega_{\rm GP})^{-1/2}$, in which $\Omega_{\rm PSF}$ is the observation angular window, related to the detector point spread function (PSF), and $\Omega_{\rm GP}$ is the solid angle of a certain region in the Galactic plane. Therefore according to the above rough evaluation, after one year observation towards the longitude interval $25°-100°$, the 5-σ minimum flux detectable by LHAASO can reach as low as $F_{\rm min} \sim 7\times10^{-16}$ photons cm^{-2} s^{-1} eV^{-1} sr^{-1} at 100 TeV, which is about 6 times lower than the extrapolation of the Fermi-DGE model at the same energy [7, 229]. Figure 22 shows the predicted DGE flux observed by one quarter LHAASO project after one year run, at Cygnus region (top) and $25° < l < 100°$, $|b| < 5°$ (bottom), respectively. It can be seen that LHAASO is very sensitive to 100 TeV γ-ray photons. Hence we could expect a better measurement for the DGE at this energy range, especially the presence of exponential cutoff at TeV energies.

(2) *Diffuse γ-ray constraints to the origin of the Fermi bubbles* Part of Fermi bubbles are in LHAASO's wide FOV. If the γ-rays stem from the interaction between the CRs and gas within the bubbles, the γ-ray spectra are anticipated to be harder and could extend to 100 TeV. According to the sensitivity of LHAASO, it can make precise measurement between 10–100 TeV and thus offer a support to the acceleration mechanism of CRs within Fermi bubbles and hadronic origin of γ-rays. Figure 23 shows the energy spectrum of the Fermi bubbles extrapolated according to the hadronic model of [230] (black solid line) and the integral sensitivity of one quarter LHAASO project (red solid line).

(3) *Diffuse γ-ray constraints to the CR knee region* The origin of the CR *knee* has been a mystery since its discovery. So far there are various models proposed to explain the break of all particle spectra at the *knee* region. However, due to the large uncertainties of the measurement of individual composition, it is hard to further testify these hypotheses. In [231], Guo *et al*. argue that the different models about the *knee* region could generate distinct DGE spectra, in which a *knee*-like structure also appears at about hundreds of TeV due to the different CR compositions around PeV energies. Thus the measurement of the DGE at hundreds of TeV could be used to distinguish the models of the *knee* region. Figure 24 shows the γ-ray spectra predicted by different *knee* models, and the grey dashed line is the expected LHAASO sensitivity.

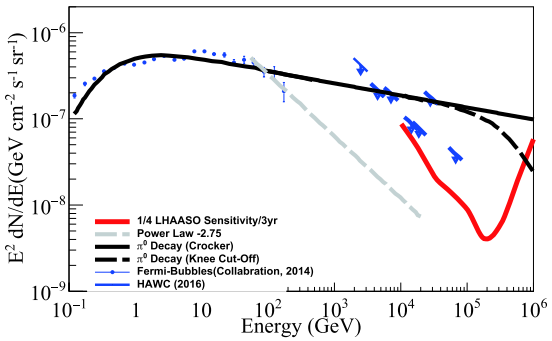

Fig. 23. (color online) The extrapolated energy spectrum of the Fermi bubbles in hadronic model (black solid line) according to [230] and the integral sensitivity of one quarter LHAASO project (red solid line).

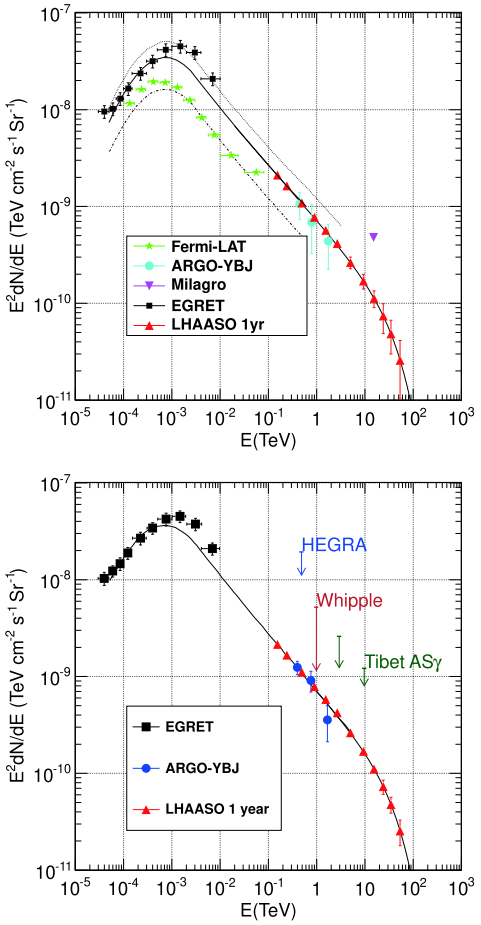

Fig. 22. (color online) The predicted DGE flux at Cygnus region (top) and $25° < l < 100°$, $|b| < 5°$ (bottom), respectively, observed by LHAASO experiment.

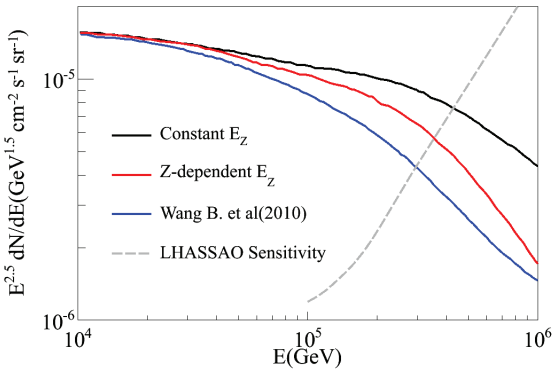

Fig. 24. (color online) The γ-ray spectra predicted by different *knee* models [231] and the LHAASO sensitivity (grey dash line).

C. Diffuse gamma-ray constraints to Galactic neutrino flux

The IceCube collaboration has recently reported the discovery of high-energy extraterrestrial neutrino flux [232]. After two years' operation, the IceCube experiment has observed 28 neutrino events between 30 TeV and 1.2 PeV, which is far above the 10.6 events evaluated from conventional atmospheric background. It declares that we have entered into a new era of neutrino astronomy. The interactions between CRs and ISM could also generate neutrinos as well as γ-rays. Thus, the neutrinos detected by the IceCube may partly originate from the Galaxy. The DGE could effectively impose restric-

tions on the origin of the Galactic neutrinos and the contribution of the Galactic neutrino flux [231, 233-236]. The measurement of the DGE above hundreds of TeV by the coming LHAASO can provide more stringent constraints.

D. Short summary

γ-ray astrophysics has made a remarkable progress. Especially recent observations of the DGE obtained by both space- and ground-based instruments have significantly changed and deepened our understanding of the origin and transport of the CRs in the Galaxy. While already being investigated at GeV energies over several decades, assessments of the DGE at TeV energies remain sparse and vast terra incognita is going to be uncovered in the future. LHAASO ground array is promising to provide more detailed observations of VHE DGE above tens of TeV and open a new window at PeV energies.

References

[1] B. S. Acharya, M. Actis *et al.*, Astroparticle Physics **43**, 3-18 (2013)
[2] A. U. Abeysekara, R. Alfaro *et al.*, Astroparticle Physics **50**, 26-32 (2013), arXiv:1306.5800
[3] M. Tluczykont, D. Hampf *et al.*, Astroparticle Physics **56**, 42-53 (2014), arXiv:1403.5688
[4] F. A. Aharonian, Astroparticle Physics **43**, 71-80 (2013)
[5] M. Ackermann *et al.*, Science **339**, 807 (2013), arXiv:1302.3307
[6] M. G. Aartsen, M. Ackermann *et al.*, Phys. Rev. Lett. **113**, 101101 (2014), arXiv:1405.5303
[7] S. Cui, Y. Liu, Y. Liu *et al.*, Astroparticle Physics **54**, 86-92 (2014)
[8] H. He (Lhaaso Collaboration), *Design highlights and status of the LHAASO project*. In "34th International Cosmic Ray Conference (ICRC2015)",, vol. 34 (2015), p. 1010
[9] M. G. Aartsen, R. Abbasi *et al.*, Phys. Rev. D **87**(6), 062002 (2013), arXiv:1210.7992
[10] B. Bartoli, P. Bernardini *et al.*, ApJ **779**(1), 27 (2013), arXiv:1311.3376
[11] R. Atkins, W. Benbow *et al.*, ApJ **608**(2), 680-685 (2004)
[12] F. Aharonian, A. G. Akhperjanian *et al.*, ApJ **636**(2), 777-797 (2006), arXiv:astro-ph/0510397
[13] R. A. Ong. *Recent Results on Galactic Sources in Cygnus by VERITAS*. In "Proceedings, 33rd International Cosmic Ray Conference (ICRC2013): Rio de Janeiro, Brazil, July 2-9, 2013 ", (2013), p. 0243. arXiv: 1307.5003. URL http://www.cbpf.br/%7Eicrc2013/papers/icrc2013-0243.pdf
[14] Tevcat catalogue. URL http://tevcat.uchicago.edu
[15] B. Bartoli, P. Bernardini *et al.*, ApJ **798**(2), 119 (2015)
[16] F. A. Aharonian, A. G. Akhperjanian *et al.*, ApJ **539**(1), 317-324 (2000)
[17] F. Aharonian, A. G. Akhperjanian *et al.*, A&A **457**(3), 899-915 (2006)
[18] J. Aleksić *et al.*, JHEA **5-6**, 30-38 (2015), arXiv:1406.6892
[19] A. A. Abdo, B. T. Allen *et al.*, ApJ **750**(1), 63 (2012)
[20] M. Tavani, A. Bulgarelli *et al.*, Science **331**(6018), 736-739 (2011)
[21] A. A. Abdo, M. Ackermann *et al.*, Science **331**(6018), 739-742 (2011)
[22] R. buehler, J. D. scargle *et al.*, ApJ **749**, 26 (2012), arXiv:1112.1979
[23] E. Striani, M. Tavani *et al.*, ApJ **765**, 52 (2013), arXiv:1302.4342
[24] S. Vernetto, Nuclear Physics B - Proceedings Supplements **239-240**, 98-103 (2013)
[25] E. Aliu *et al.*, Astrophys. J. **781**(1), L11 (2014), arXiv:1309.5949
[26] A. Abramowski *et al.* (H.E.S.S. Collaboration), A&A **562**, L4 (2014)
[27] F. A. Aharonian, A. G. Akhperjanian *et al.*, A&A **531**, C1 (2011)
[28] A. A. Abdo, M. Ackermann *et al.*, ApJ **734**(1), 28 (2011), arXiv:1103.5727
[29] H. Abdalla *et al.* (H.E.S.S. Collaboration), Astron. Astrophys. **612**, A7 (2018), arXiv:1611.01863
[30] M. L. Ahnen, S. Ansoldi *et al.*, Mon. Not. R. Astron.Soc. **472**(3), 2956-2962 (2017), arXiv:1707.01583
[31] A. Abramowski *et al.* (H.E.S.S. Collaboration), Astron. Astrophys. **612**, A4 (2018), arXiv:1601.04461
[32] V. A. Acciari, E. Aliu *et al.*, ApJ **730**(2), L20 (2011)
[33] J. Albert, E. Al iu *et al.*, A&A **474**(3), 937-940 (2007)
[34] J. Aleksi′c, E. A. Alvarez *et al.*, A&A **541**, A13 (2012)
[35] V. A. Acciari, E. Aliu *et al.*, ApJ **698**(2), L133-L137 (2009)
[36] F. Brun, M. de Naurois *et al. Discovery of VHE gammaray emission from the W49 region with H.E.S.S.* In "25th Texas Symposium on Relativistic Astrophysics", (2010), p.201. arXiv: 1104.5003
[37] V. A. Acciari, E. Aliu *et al.*, The Astrophysical Journal **703**(1), L6-L9 (2009)
[38] S. Archambault, A. Archer *et al.*, ApJ **836**(1), 23 (2017), arXiv:1701.06740
[39] Y. Liu, Z. Cao *et al.*, ApJ **826**(1), 63 (2016), arXiv:1605.05472
[40] F. Acero, M. Ackermann *et al.*, ApJS **218**, 23 (2015), arXiv:1501.02003
[41] C. L. Bhat, M. R. Issa, C. J. Mayer *et al.*, Nature **314**(6011), 515-517 (1985)
[42] A. M. Hillas, Journal of Physics G: Nuclear and Particle Physics **31**(5), R95-R131 (2005)
[43] B. Katz and E. Waxman, Journal of Cosmology and Astroparticle Physics **2008**(01), 018 (2008)
[44] W. Tian and J. Zhang, Science China Physics, Mechanics, and Astronomy **56**(8), 1443-1453 (2013), arXiv:1301.6824
[45] Z. Mao amd Y.-W. Yu, Research in Astronomy and Astrophysics **13**(8), 952-960 (2013)
[46] G. Joncas and L. A. Higgs, Astronomy and Astrophysics Suppl.Series **82**, 113-144 (1990)
[47] S. Pineault and G. Joncas, ApJ **120**(6), 3218-3225 (2000)
[48] R. C. Hartman, D. L. Bertsch *et al.*, ApJS **123**(2), 79-202 (1999)
[49] Q. Yuan, S. Liu *et al.*, ApJ **735**(2), 120 (2011)
[50] Q. Yuan, S. Liu, and X. Bi, ApJ **761**(2), 133 (2012)

[51] H. Li and Y. Chen, Mon. Not. R. Astron. Soc. **409**(1), L35-L38 (2010), arXiv:1009.0894
[52] H. Li and Y. Chen, Mon. Not. R. Astron. Soc. **421**(2), 935-942 (2012), arXiv:1108.4541
[53] Y. Uchiyama, F. A. Aharonian *et al*., Nature **449**, 576 (2007)
[54] A. A. Abdo, M. Ackermann *et al*., ApJ **708**, 1254-1267 (2010), arXiv:0911.2412
[55] A. A. Abdo, M. Ackermann *et al*., Science **327**(5969), 1103-1106 (2010)
[56] A. Abramowski *et al*. (H.E.S.S. Collaboration), A&A **531**, A81 (2011)
[57] L. Saha, T. Ergin *et al*., Astron. Astrophys. **563**, A88 (2014), arXiv:1401.5626
[58] R. Hanbury Brown and C. Hazard, Mon. Not. R. Astron.Soc. **113**, 123 (1953)
[59] J. R. Dickel, W. J. M. van Breugel, and R. G. Strom, ApJ **101**, 2151 (1991)
[60] W. W. Tian and D. A. Leahy, ApJL **729**(2), L15 (2011), arXiv:1012.5673
[61] U. Hwang, R. Petre, A. E. Szymkowiak *et al*., Journal of Astrophysices and Astronomy **23**, 81 (2002)
[62] A. Bamba, R. Yamazaki, and J. S. Hiraga, ApJ **632**, 294-301 (2005), arXiv:astro-ph/0506331
[63] W. Stroman and M. Pohl, ApJ **696**, 1864-1870 (2009), arXiv:0902.1701
[64] S. Katsuda, R. Petre *et al*., ApJ **709**(2), 1387-1395 (2010)
[65] F. Giordano, M. Naumann-Godo *et al*., ApJ **744**(1), L2 (2011)
[66] S. R. Kelner, F. A. Aharonian, and V. V. Bugayov, Phys. Rev. D **74**, 034018 (2006)
[67] V. A. Acciari, E. Aliu *et al*., ApJ **709**, L163-L167 (2010), arXiv:1001.2590
[68] F. Aharonian, A. Akhperjanian *et al*., A&A **370**(1), 112-120 (2001)
[69] Y. Yuan, S. Funk *et al*., ApJ **779**(2), 117 (2013)
[70] A. A. Abdo, M. Ackermann *et al*., ApJ **712**(1), 459-468 (2010)
[71] J. Albert *et al*., ApJ **664**, L87-L90 (2007)
[72] B.-C. Koo, K.-T. Kim, and F. D. Seward, ApJ **447**, 211 (1995)
[73] W. W. Tian, D. A. Leahy, ApJL **769**(1), L17 (2013), arXiv:1305.0325
[74] M. F. Zhang, W. W. Tian *et al*., ApJ **849**(2), 147 (2017), arXiv:1710.04770
[75] I. Reichardt, E. Carmona, J. Krause *et al*. (MAGIC Collaboration), Memorie della Società Astronomica Italiana **82**, 735 (2011)
[76] A. A. Abdo, M. Ackermann *et al*., Nature **462**, 331 (2009)
[77] A. Fiasson, V. Marandon, R. Chaves *et al*. *Discovery of a vhe gamma-ray source in the w51 region*. In "31st International Cosmic Ray Conference (ICRC 2009)",, vol. ICRC 2009, (Lodz, Poland2009), p. 1. URL http://hal.in2p3.fr/in2p3-00432338
[78] X. Zhang and S. Liu, ApJL **874**(1), 98 (2019), arXiv:1903.02373
[79] Y. Zhang, S. Liu, and Q. Yuan, ApJL **844**(1), L3 (2017), arXiv:1707.00262
[80] W. R. Binns, M. H. Israel *et al*., Science **352**, 677-680 (2016)
[81] F. Acero, M. Ackermann *et al*., The Astrophysical Journal Supplement Series **223**(2), 26 (2016)
[82] R. Yang, F. Aharonian, and C. Evoli, Phys. Rev. D **93**, 123007 (2016)
[83] E.Parizot, A.Marcowith *et al*., A&A **424**(3), 747-760 (2004)
[84] P. L. Nolan, A. A. Abdo *et al*., The Astrophysical Journal Supplement Series **199**(2), 31 (2012)
[85] A. A. Abdo, B. Allen *et al*., ApJ **658**(1), L33-L36 (2007)
[86] A. A. Abdo, B. Allen *et al*., ApJ **664**(2), L91-L94 (2007)
[87] M. Ackermann, M. Ajello *et al*., Science **334**(6059), 1103-1107 (2011)
[88] B. Bartoli, P. Bernardini *et al*., ApJ **790**(2), 152 (2014)
[89] P. G. Mezger, J. Schraml, and Y. Terzian, ApJ **150**, 807 (1967)
[90] A. W. Sievers, P. G. Mezger *et al*., Astron. Astrophys. **251**, 231-244 (1991)
[91] R. Simon, J. M. Jackson *et al*., ApJ **551**(2), 747-763 (2001)
[92] C. G. D. Pree, D. M. Mehringer, and W. M. Goss, ApJ **482**(1), 307-333 (1997)
[93] R. Genzel, D. Downes *et al*., Astron.Astrophys. **66**, 13-29 (1978)
[94] C. R. Gwinn, J. M. Moran, and M. J. Reid, ApJ **393**, 149-164 (1992)
[95] T.-C. Peng, F. Wyrowski *et al*., A&A **520**, A84 (2010)
[96] Rui-zhi Yang, Aharonian, Felix, A&A **600**, A107 (2017)
[97] A. G. Muslimov and A. K. Harding, ApJ **606**, 1143-1153 (2004), arXiv:astro-ph/0402462
[98] A. McCann, International Cosmic Ray Conference **7**, 208 (2011), arXiv:1110.4352
[99] S. Ansoldi, L. A. Antonelli *et al*., A&A **585**, A133 (2016)
[100] G. C. K. Leung, J. Takata *et al*., ApJ **797**, L13 (2014), arXiv:1410.5208
[101] Y. Xing and Z. Wang, ApJ **831**(2), 143 (2016), arXiv:1604.08710
[102] M. Lyutikov, Astronomische Nachrichten **335**(3), 227-233 (2014)
[103] A. K. Harding and C. Kalapotharakos, ApJ **811**(1), 63 (2015), arXiv:1508.06251
[104] J. Takata, C. W. Ng, and K. S. Cheng, Mon. Not. R. Astron. Soc. **455**, 4249-4266 (2016), arXiv:1511.06542
[105] M. Ackermann, M. Ajello *et al*., ApJS **209**, 11 (2013), arXiv:1303.2908
[106] B. M. Gaensler and P. O. Slane, Annual Review of Astronomy and Astrophysics **44**(1), 17-47 (2006)
[107] A. Lemiere, P. Slane, B. M. Gaensler *et al*., ApJ **706**, 1269-1276 (2009), arXiv:0910.2652
[108] J. Fang and L. Zhang, Astron. Astrophys. **515**, A20 (2010), arXiv:1003.1656
[109] J. Martín, D. F. Torres, and N. Rea, Mon. Not. R. Astron. Soc. **427**(1), 415-427 (2012), arXiv:1209.0300
[110] T. Linden, K. Auchettl *et al*., prd **96**(10), 103016 (2017), arXiv:1703.09704
[111] T. Sudoh, T. Linden, and J. F. Beacom, Phys. Rev. D **100**(4), 043016 (2019), arXiv:1902.08203
[112] G. Giacinti, A. M. W. Mitchell *et al*., Astron. Astrophys. **636**, A113 (2020), arXiv:1907.12121
[113] F. Acero, M. Ackermann, *et al*., ApJ **773**(1), 77 (2013)
[114] M. Amenomori, Y. W. Bao *et al*., Phys. Rev. Lett. **123**(5), 051101 (2019), arXiv:1906.05521
[115] A. U. Abeysekara, A. Albert *et al*., ApJ **881**(2), 134 (2019), arXiv:1905.12518
[116] A. U. Abeysekara, A. Albert *et al*., Phys. Rev. Lett. **124**(2), 021102 (2020)
[117] A. M. Hillas, Annual Review of Astronomy and

Astrophysics **22**(1), 425-444 (1984)
[118] K. S. Cheng, T. Cheung *et al.*, Journal of Physics G Nuclear Physics **16**, 1115-1121 (1990)
[119] Y. Ohira, S. Kisaka, and R. Yamazaki, Mon. Not. Roy. Astron. Soc. **478**(1), 926-931 (2018), arXiv:1702.05866
[120] H. Bartko and W. Bednarek, Monthly Notices of the Royal Astronomical Society **385**(3), 1105-1109 (2008)
[121] L. Zhang and X. C. Yang, ApJ **699**(2), L153-L156 (2009)
[122] H. Li, Y. Chen, and L. Zhang, Monthly Notices of the Royal Astronomical Society: Letters **408**(1), L80-L84 (2010)
[123] A. Coerver, P. Wilcox *et al.*, ApJ **878**(2), 126 (2019), arXiv:1905.07327
[124] Y. Xin, H. Zeng *et al.*, ApJ **885**(2), 162 (2019), arXiv:1907.04972
[125] S. Liu, H. Zeng, Y. Xin *et al.*, ApJL **897**(2), L34 (2020), arXiv:2006.14946
[126] C. Guépin, B. Cerutti, and K. Kotera, Astron. Astrophys. **635**, A138 (2020), arXiv:1910.11387
[127] X. Zhang, Y. Chen, J. Huang *et al.*, Mon. Not. R. Astron. Soc. **497**(3), 3477-3483 (2020), arXiv:2008.01309
[128] A. A. Abdo, B. T. Allen *et al.*, ApJ **700**(2), L127-L131 (2009)
[129] A. U. Abeysekara, A. Albert *et al.*, Science **358**(6365), 911 (2017)
[130] M. L. Ahnen, S. Ansoldi *et al.*, A&A **591**, A138 (2016)
[131] O. Adriani, G. C. Barbarino *et al.*, Nature **458**, 607-609 (2009), arXiv:0810.4995
[132] M. Ackermann *et al.*, Phys. Rev. Lett. **108**, 011103 (2012), arXiv:1109.0521
[133] M. Aguilar *et al.*, Phys. Rev. Lett. **110**, 141102 (2013)
[134] D. Hooper, P. Blasi, and P. D. Serpico, Journal of Cosmology and Astroparticle Physics **2009**(01), 025-025 (2009)
[135] D. Malyshev, I. Cholis, and J. Gelfand, Phys. Rev. D **80**, 063005 (2009)
[136] H. Yüksel, M. D. Kistler, and T. Stanev, Phys. Rev. Lett. **103**, 051101 (2009)
[137] T. Linden and S. Profumo, ApJ **772**, 18 (2013), arXiv:1304.1791
[138] D. Hooper, I. Cholis, T. Linden *et al.*, Phys. Rev. D **96**(10), 103013 (2017), arXiv:1702.08436
[139] J. P. W. Verbiest, J. M. Weisberg *et al.*, ApJ **755**, 39 (2012), arXiv:1206.0428
[140] B. Posselt, G. G. Pavlov, P. O. Slane *et al.*, ApJ **835**(1), 66 (2017), arXiv:1611.03496
[141] L. Bîrzan, G. G. Pavlov, and O. Kargaltsev, ApJ **817**(2), 129 (2016), arXiv:1511.03846
[142] M. Aguilar, L. Ali Cavasonza *et al.*, Phys. Rev. Lett. **117**(23), 231102 (2016)
[143] R. Trotta, G. Jóhannesson *et al.*, ApJ **729**, 106 (2011), arXiv:1011.0037
[144] P.-F. Yin, Z.-H. Yu, Q. Yuan *et al.*, Phys. Rev. D **88**(2), 023001 (2013), arXiv:1304.4128
[145] R. López-Coto, R. D. Parsons, J. A. Hinton *et al.*, Phys. Rev. Lett. **121**(25), 251106 (2018), arXiv:1811.04123
[146] A. M. Bykov, A. E. Petrov *et al.*, ApJ **876**(1), L8 (2019), arXiv:1904.09430
[147] K. Fang, X.-J. Bi, and P.-F. Yin, ApJ **884**(2), 124 (2019), arXiv:1906.08542
[148] K. Fang, X.-J. Bi, P.-F. Yin *et al.*, ApJ **863**, 30 (2018), arXiv:1803.02640
[149] C. Evoli, T. Linden, and G. Morlino, Phys. Rev. D **98**(6), 063017 (2018), arXiv:1807.09263
[150] J. Faherty, F. M. Walter, and J. Anderson, Astrophy. and SSci. **308**(1-4), 225-230 (2007)
[151] K. Fang, X.-J. Bi, and P.-F. Yin, Mon. Not. R. Astron. Soc. **488**(3), 4074-4080 (2019), arXiv:1903.06421
[152] R.-Y. Liu, H. Yan, and H. Zhang, Phys. Rev. Lett. **123**(22), 221103 (2019), arXiv:1904.11536
[153] C. Brisbois nad H. Zhou. *First Galactic Survey of EnergyDependent Diffusion by HAWC*. In "36th International Cosmic Ray Conference (ICRC2019) ",, *International Cosmic Ray Conference*, vol. 36 (**2019**), p. 640
[154] R. N. Manchester, G. B. Hobbs, A. Teoh *et al.*, ApJ **129**, 1993-2006 (2005), arXiv:astro-ph/0412641
[155] G. Dubus, The Astronomy and Astrophysics Review **21**(1), 64 (2013)
[156] A. G. Lyne, B. W. Stappers *et al.*, Mon. Not. R. Astron. Soc. **451**, 581-587 (2015), arXiv:1502.01465
[157] R. Zanin, A. Fernández-Barral *et al.*, Astron. Astrophys. **596**, A55 (2016), arXiv:1605.05914
[158] M. Tavani, A. Bulgarelli *et al.*, Nature **462**, 620-623 (2009), arXiv:0910.5344
[159] A. Loh, S. Corbel *et al.*, Mon. Not. R. Astron. Soc. **462**, L111-L115 (2016), arXiv:1607.06239
[160] A. A. Abdo, M. Ackermann *et al.*, ApJ **723**, 649-657 (2010), arXiv:1008.3235
[161] P. H. T. Tam, R. H. H. Huang *et al.*, ApJ **736**(1), L10 (2011)
[162] A. A. Abdo, M. Ackermann *et al.*, ApJ **736**(1), L11 (2011)
[163] A. O 'Faolain de Bhroithe (VERITAS Collaboration), "VERITAS observations of exceptionally bright TeV flares from LS I +61◦ 303". arXiv: 1508.06800
[164] M. G. Aartsen, M. Ackermann *et al.*, ApJ **807**(1), 46 (2015)
[165] J. M. Paredes, W. Bednarek *et al.*, Astroparticle Physics **43**, 301-316 (2013), arXiv:1210.3215
[166] M. Clavel, R. Terrier *et al.*, Astron. Astrophys. **558**, A32 (2013), arXiv:1307.3954
[167] M. Su, T. R. Slatyer, and D. P. Finkbeiner, ApJ **724**, 1044-1082 (2010), arXiv:1005.5480
[168] F. Aharonian and A. Neronov, ApJ **619**, 306-313 (2005), arXiv:astro-ph/0408303
[169] K. Dodds-Eden, D. Porquet *et al.*, ApJ **698**, 676-692 (2009), arXiv:0903.3416
[170] S. Markoff, H. Falcke, F. Yuan *et al.*, Astron. Astrophys. **379**, L13-L16 (2001), arXiv:astro-ph/0109081
[171] R. P. Eatough, H. Falcke *et al.*, Nature **501**, 391-394 (2013), arXiv:1308.3147
[172] K. Tsuchiya, R. Enomoto *et al.*, ApJL **606**, L115-L118 (2004), arXiv:astro-ph/0403592
[173] K. Kosack, H. M. Badran *et al.*, ApJL **608**, L97-L100 (2004), arXiv:astro-ph/0403422
[174] A. W. Smith (for the VERITAS Collaboration), "VERITAS Observations of The Galactic Center Ridge". arXiv: 1508.06311
[175] F. Aharonian, A. G. Akhperjanian *et al.*, Astron. Astrophys. **425**, L13-L17 (2004), arXiv:astro-ph/0406658
[176] F. Aharonian, A. G. Akhperjanian *et al.*, Nature **439**, 695-698 (2006), arXiv:astro-ph/0603021
[177] F. Aharonian, A. G. Akhperjanian *et al.*, Phys. Rev. Lett. **97**(22), 221102 (2006), arXiv:astro-ph/0610509
[178] F. Aharonian, A. G. Akhperjanian *et al.*, Astron. Astrophys. **492**, L25-L28 (2008), arXiv:0812.3762

[179] J. Albert, E. Aliu *et al*., ApJL **638**, L101-L104 (2006), arXiv:astro-ph/0512469
[180] A. Abramowski *et al*. (HESS Collaboration), Nature **531**, 476-479 (2016), arXiv:1603.07730
[181] F. Aharonian, A. G. Akhperjanian *et al*., Astron. Astrophys. **503**, 817-825 (2009), arXiv:0906.1247
[182] S. Gabici, F. A. Aharonian, and P. Blasi, Astrophysics and Space Science **309**(1), 365-371 (2007)
[183] F. Aharonian, A. G. Akhperjanian *et al*., Phys. Rev. Lett. **101**, 261104 (2008)
[184] A. W. Strong, I. V. Moskalenko, and V. S. Ptuskin, Annual Review of Nuclear and Particle Science **57**(1), 285-327 (2007)
[185] T. M. Dame, H. Ungerechts, R. S. Cohen *et al*., ApJ, **322**, 706 (1987) DOI: 10.1086/165766, Provided by the SAO/NASA Astrophysics Data System
[186] F. A. Aharonian, Space Science Reviews **99**, 187-196 (2001), arXiv:astro-ph/0012290
[187] S. Casanova, F. A. Aharonian *et al*., PASJ **62**, 769 (2010), arXiv:0904.2887
[188] G. Pedaletti, D. F. Torres *et al*., Astron. Astrophys. **550**, A123 (2013), arXiv:1301.5240
[189] M. Ackermann, M. Ajello *et al*., ApJ **755**(1), 22 (2012)
[190] M. Ackermann, M. Ajello *et al*., ApJ **756**(1), 4 (2012)
[191] A. Neronov, D. V. Semikoz, and A. M. Taylor, Phys. Rev. Lett. **108**, 051105 (2012)
[192] Rui-zhi Yang, de Oña Wilhelmi, Emma, Aharonian, A&A **566**, A142 (2014)
[193] Yang, Rui-zhi, Jones, David I., Aharonian, Felix, A&A **580**, A90 (2015)
[194] M. Aguilar, D. Aisa, B. Alpat *et al*., Phys. Rev. Lett. **114**(17), 171103 (2015)
[195] O. Adriani, G. C. Barbarino *et al*., Science **332**(6025), 69-72 (2011)
[196] A. D. Panov, J. H. Adams *et al*., Bulletin of the Russian Academy of Sciences: Physics **73**(5), 564-567 (2009)
[197] W. R. Binns, M. E. Wiedenbeck *et al*., ApJ **634**, 351-364 (2005), arXiv:astro-ph/0508398
[198] J. Bally. *Overview of the Orion Complex*, vol. 4, chap.Overview of the Orion Complex, (Astronomical Society of the Pacific Monograph Publications, 2008). ISBN 978-1-58381-670-7, p. 459
[199] A. Abramowski, F. Aharonian *et al*., ApJ **794**(1), L1 (2014)
[200] R. C. G. Chaves, M. Renaud, M. Lemoine-Goumard *et al*., American Institute of Physics Conference Series **1085**, 372-375 (2008)
[201] A. U. Abeysekara, R. Alfaro *et al*., ApJ **817**(1), 3 (2016)
[202] M. S. Longair. *High Energy Astrophysics*, (Cambridge University Press, 2011). ISBN 978052175618
[203] W. L. Kraushaar, G. W. Clark *et al*., ApJ **177**, 341 (1972)
[204] C. E. Fichtel, R. C. Hartman *et al*., ApJ **198**, 163-182 (1975)
[205] G. F. Bignami, G. Boella *et al*., Space Science Instrumentation **1**, 245-268 (1975)
[206] A. W. Strong, K. Bennett *et al*., Astron. Astrophys. **292**, 82-91 (1994)
[207] S. C. Kappadath, J. Ryan *et al*., Astronomy and Astrophysics Supplement Series **120**, 619-622 (1996)
[208] R. L. Kinzer, G. V. Jung *et al*., ApJ **475**, 361-372 (1997)
[209] S. D. Hunter, D. L. Bertsch *et al*., ApJ **481**, 205-240 (1997)
[210] M. Ackermann, M. Ajello *et al*., ApJ **750**(1), 3 (2012), arXiv:1202.4039
[211] M. Ajello, A. Albert *et al*., ApJ **819**, 44 (2016), arXiv:1511.02938
[212] L. Bouchet, E. Jourdain *et al*., ApJ **679**, 1315-1326 (2008), arXiv:0801.2086
[213] L. Bouchet, A. W. Strong *et al*., ApJ **739**, 29 (2011), arXiv:1107.0200
[214] S. LeBohec, I. H. Bond *et al*., ApJ **539**, 209-215 (2000), arXiv:astro-ph/0003265
[215] F. A. Aharonian, A. G. Akhperjanian *et al*., Astron. Astrophys. **375**, 1008-1017 (2001)
[216] A. Abramowski, F. Aharonian *et al*., Phys. Rev. D **90**, 122007 (2014), arXiv:1411.7568
[217] B. Bartoli, P. Bernardini *et al*., ApJ **806**, 20 (2015), arXiv:1507.06758
[218] A. W. Strong, I. V. Moskalenko, and O. Reimer, ApJ **613**, 962-976 (2004), arXiv:astro-ph/0406254
[219] A. W. Strong, I. V. Moskalenko *et al*., Astron. Astrophys. **422**, L47-L50 (2004), arXiv:astro-ph/0405275
[220] T. Delahaye, A. Fiasson, M. Pohl *et al*., Astron. Astrophys. **531**, A37 (2011), arXiv:1102.0744
[221] A. A. Abdo, M. Ackermann *et al*., Phys. Rev. Lett. **103**, 251101 (2009), arXiv:0912.0973
[222] X.-J. Bi, J. Zhang *et al*., Phys. Lett. B **668**, 87-92 (2008), arXiv:astro-ph/0611783
[223] J. Zhang, Q. Yuan, and X.-J. Bi, ApJ **720**, 9-19 (2010), arXiv:0908.1236
[224] Y.-Q. Guo, H.-B. Hu, and Z. Tian, Chin. Phys. C **40**, 115001 (2016), arXiv:1412.8590
[225] R. Atkins, W. Benbow *et al*., Phys. Rev. Lett. **95**, 251103 (2005), arXiv:astro-ph/0502303
[226] F. Aharonian, J. Buckley, T. Kifune *et al*., Reports on Progress in Physics **71**, 096901 (2008)
[227] M. Ackermann, A. Albert *et al*., ApJ **793**, 64 (2014), arXiv:1407.7905
[228] I. A. Grenier, J. H. Black, and A. W. Strong, Annual Review of Astronomy and Astrophysics **53**, 199-246 (2015)
[229] G. Di Sciascio (LHAASO Collaboration), Nuclear and Particle Physics Proceedings **279**, 166-173 (2016), arXiv:1602.07600
[230] R. M. Crocker and F. Aharonian, Phys. Rev. Lett. **106**, 101102 (2011), arXiv:1008.2658
[231] Y. Q. Guo, H. B. Hu *et al*., ApJ **795**, 100 (2014), arXiv:1312.7616
[232] M. G. Aartsen, R. Abbasi *et al*., Phys. Rev. Lett. **111**, 021103 (2013), arXiv:1304.5356
[233] S. Razzaque, Phys. Rev. D **88**, 081302 (2013), arXiv:1309.2756
[234] M. Ahlers and K. Murase, Phys. Rev. D **90**, 023010 (2014), arXiv:1309.4077
[235] A. Neronov, D. Semikoz, and C. Tchernin, Phys. Rev. D **89**, 103002 (2014), arXiv:1307.2158
[236] D. Gaggero, D. Grasso *et al*., ApJ **815**, L25 (2015), arXiv:1504.00227